

Hydrocarbon-Bridged Methylmethoxysilanes as new Co-condensation Agents for the Sol–Gel Process of the Rhodium(I) Complex $\text{ClRh}(\text{CO})(\text{P}\sim\text{O})_2$ Containing the Ligand $\text{PhP}(\text{CH}_2\text{CH}_2\text{OCH}_3)(\text{CH}_2)_3\text{Si}(\text{OCH}_3)_3$ ^{1–3}

Ekkehard Lindner,^{*,†} Theodor Schneller,[†] Hermann A. Mayer,^{†,§}
Helmut Bertagnolli,[‡] Teja S. Ertel,[‡] and Wolfgang Hörner[‡]

*Institut für Anorganische Chemie der Universität, Auf der Morgenstelle 18,
D-72076 Tübingen, and Institut für Physikalische Chemie der Universität,
Pfaffenwaldring 55, D-70569 Stuttgart, Germany*

Received November 5, 1996. Revised Manuscript Received April 29, 1997[®]

New hydrocarbon bridged co-condensation agents of the type $\text{MeSi}(\text{OMe})_2(\text{CH}_2)_z(\text{MeO})_z\text{-SiMe}$ [$\mathbf{1}(\text{D}^0\text{-C}_z\text{-D}^0)$, $z = \text{length of the flexible bridging group } (z = 6, 8, 14)$] were synthesized and polycondensed to give the polysiloxanes $\mathbf{1}(\text{D}^i\text{-C}_z\text{-D}^i)$. These monomers were employed in variable amounts y in the sol–gel processing of the monomeric ether–phosphine ligand $\text{PhP}(\text{CH}_2\text{CH}_2\text{OMe})(\text{CH}_2)_3\text{Si}(\text{OMe})_3$ [$\mathbf{2}(\text{T}^0)$] and its P-coordinated trimethoxysilyl-(T)-functionalized rhodium(I) complex $\text{ClRh}(\text{CO})(\text{P}\sim\text{O})_2$ [$\mathbf{3}(\text{T}^0)_2$] to yield the polysiloxane-bound ether–phosphine ligands $\mathbf{2}(\text{T}^n)(\text{D}^i\text{-C}_z\text{-D}^i)$ and the rhodium complexes $\mathbf{3}(\text{T}^n)_2(\text{D}^i\text{-C}_z\text{-D}^i)_y$ [$\text{O}\sim\text{P}$: η^1 -P-coordinated ether–phosphine ligand; $y = \text{number of co-condensed D-C}_z\text{-D molecules}$; D = D-type silicon atom (two oxygen neighbors), T = T-type silicon atom (three oxygen neighbors); $i, n = \text{number of Si-O-Si bonds}$; $i = 0\text{--}2$; $n = 0\text{--}3$]. The relative amounts of T and D silyl species and the degree of condensation were determined by ²⁹Si CP/MAS NMR spectroscopic investigations. The polysiloxanes $\mathbf{1}(\text{D}^i\text{-C}_z\text{-D}^i)$ which are regarded as “organofunctionalized Q analogues” display a higher degree of condensation than their Q counterpart [Q = Q-type silicon atom (four oxygen neighbors)]. The highest degrees of condensation of the D groups were obtained for the D–C₁₄–D polymer and the F–T/D–C₁₄–D copolymers [F = (Ph)P(CH₂CH₂OMe)(CH₂)₃– (**2**), [ClRh(CO)]_{1/2}(Ph)P(CH₂CH₂OMe)(CH₂)₃– (**3**)]. ³¹P and ¹³C CP/MAS NMR spectroscopic studies give evidence that the ligand and the geometry of the complex is preserved during the entire sol–gel process. In addition an EXAFS spectroscopic analysis of the complex $\mathbf{3}(\text{T}^n)_2$ gave a more detailed description of its structure. ³¹P CP/MAS NMR relaxation time studies (T_{1P} , T_{PH} , $T_{1\rho H}$), 2D WISE NMR experiments, and the line widths of the ³¹P CP/MAS NMR spectra were applied for dynamic investigations. The noncomplexed ether–phosphine ligand in the F–T/D–C_z–D copolymers is more mobile than that in the F–T/Q copolymer $\mathbf{2}(\text{T}^n)(\text{Q}^k)_2$ [$k = \text{number of Si-O-Si bonds}$; $k = 0\text{--}4$]. The P-coordination of only two ether–phosphines in the complex leads to an additional cross-linking in the matrixes. Thereby the ligands become more rigid due to strong phosphorus–rhodium bonds.

Introduction

The immobilization of reactive centers has evolved into an area of intensive research for reasons which combine, e.g., the advantages of homogeneous with those of heterogeneous catalysis.^{4,5} In contrast to the surface coverage of silica,^{6–8} the sol–gel process offers

unique possibilities to prepare organic–inorganic hybrid materials with excellent properties, for example: (i) reduced leaching of functional groups, (ii) high degrees of condensation, and (iii) higher loading of catalysts.^{9,10} Simultaneous cohydrolysis and subsequent polycondensation of trimethoxysilyl-(T)-functionalized transition-metal complexes with different alkoxysilanes $R_n\text{Si}(\text{OR})_{4-n}$ ($n = 0\text{--}2$) provides polymers with diverse properties ranging from inorganic silicates (polar, high surface area ($n = 0$)) to organically modified linear polysiloxanes (nonpolar, low surface area ($n = 2$)).^{10–12}

* To whom correspondence should be sent.

[†] Institut für Anorganische Chemie der Universität Tübingen.

[‡] Institut für Physikalische Chemie der Universität Stuttgart.

[§] E-mail: hermann.mayer@uni-tuebingen.de.

[®] Abstract published in *Advance ACS Abstracts*, June 15, 1997.

(1) Dedicated to Professor W. Siebert on the occasion of his 60th birthday.

(2) Supported Organometallic Complexes Part 12. Part 11: Lindner, E.; Jäger, A.; Schneller, T.; Mayer, H. A. *Chem. Mater.* **1997**, *9*, 81.

(3) Parts of this work were presented at the 17th Conference and Workshop on *Magnetic Resonance and the Structure of Matter*, Gosen, Germany, 1995.

(4) Hartley, F. R. *Supported Metal Complexes*, D. Reidel Publishing Co.: Dordrecht, 1985.

(5) Deschler, U.; Kleinschmit, P.; Panster, P. *Angew. Chem., Int. Ed. Engl.* **1986**, *25*, 236.

(6) Sindorf, D. W.; Maciel, G. E. *J. Am. Chem. Soc.* **1983**, *105*, 3767.

(7) Bayer, E.; Albert, K.; Reiners, J.; Nieder, M.; Müller, D. *J. Chromatogr.* **1983**, *264*, 197.

(8) Blümel, J. *Inorg. Chem.* **1994**, *33*, 5050.

(9) Brinker, C. J.; Scherer, G. W. *Sol Gel Science*, Academic Press: London, 1990.

(10) Lindner, E.; Kemmler, M.; Mayer, H. A.; Wegner, P. *J. Am. Chem. Soc.* **1994**, *116*, 348.

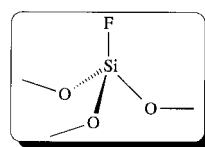
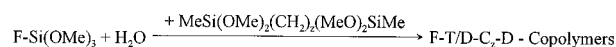
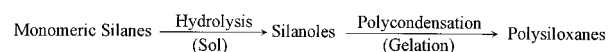
(11) Schubert, U.; Egger, C.; Rose, K.; Alt, C. *J. Mol. Catal.* **1989**, *55*, 330.

These novel organometallic–inorganic hybrid materials are considered to be stationary phases consisting of the matrix (polysiloxane), the spacer ($-\text{CH}_2-\text{CH}_2-$) and the reactive center (metal complex). In the presence of a mobile phase (solvent, gaseous, or liquid reactant) the penetration of the stationary phase on a molecular level takes place. This state is called interphase since no homogeneous mixture is formed.¹³ Such interphases allow substrates an easy access to the reactive centers, if certain preconditions are fulfilled. This was recently proved by stoichiometric reactions.¹⁴ The accessibility of the reactive centers is determined either by high surface areas or by sufficient swelling abilities of the stationary phase. Despite this promising concept the activities and selectivities obtained by various types of supported catalysts are still not satisfactory and therefore technically not applicable yet. Responsible for these problems are the restricted mobilities of the active centers due to their support.¹⁵ It is obvious that the activities and selectivities in the homogeneous catalysis are determined by high mobilities of the reactive centers and the substrates. If the mobilities of the immobilized complexes will increase, it is supposed that a more solution-like behavior is achieved combined with higher turnover frequencies and selectivities. Therefore it is desirable to improve the dynamic properties of the stationary phases.

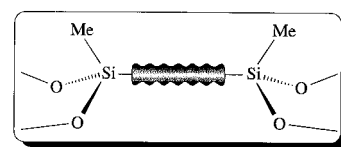
Recently it was shown that the type of co-condensation agents and the length of spacers in the immobilized ligands of the type $\text{PhP}(\text{CH}_2\text{CH}_2\text{OME})(\text{CH}_2)_x\text{Si}(\text{OME})_3$ ($x = 3, 6, 8$) strongly influence their mobilities and the structures of the organometallic–inorganic hybrid polymer frameworks.^{2,12} F–T/D blends (for definition of F see ref 16), which were built up from the ligand $\text{PhP}(\text{CH}_2\text{CH}_2\text{OME})(\text{CH}_2)_8\text{Si}(\text{OME})_3$ co-condensed with $\text{Me}_2\text{Si}(\text{OEt})_2$ (\mathbf{D}^0), showed the highest flexibilities, but the T/D ratio in F–T/D copolymers has an upper limit of 1:1.5.¹² Thus the metal complex density within the F–T/D polymer is not controllable and therefore the reactivity cannot be adjusted like in the F–T/T and F–T/Q polysiloxane matrixes. For that reason they seem to be unsuitable for the use as stationary phases in interphases.

Bis(trialkoxo) and bis(diethoxy)methyl silylated organic precursors were successfully employed to generate a variety of hybrid organic–inorganic polysiloxanes generally presenting high surface areas.^{17–21} These bridged polymers form highly condensed networks with

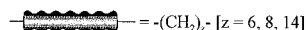
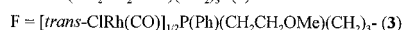
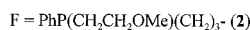
Scheme 1



F-T
functionalized
complex or ligand



D-C_z-D
co-condensate



T: T type silicon atom (three oxygen neighbors)

D: D type silicon atom (two oxygen neighbors)

the organic fragment securely bound by two covalent Si–C bonds. Although the identity of the organic fragment is easy to modify, these bridged alkoxy silanes have never been used as co-condensation agents in the sol–gel process of trimethoxysilyl-(T)-functionalized transition-metal complexes.

Here we wish to report the synthesis of the bisilylated D-functionalized co-condensation agents $\text{MeSi}(\text{OME})_2(\text{CH}_2)_z(\text{MeO})_2\text{SiMe}$ ($\mathbf{D}^0\text{-C}_z\text{-D}^0$)²² ($z = 6, 8, 14$; Scheme 1) and their use in the sol–gel process of the T-functionalized ether–phosphine $\text{PhP}(\text{CH}_2\text{CH}_2\text{OME})(\text{CH}_2)_3\text{Si}(\text{OME})_3$ and its rhodium(I) complex $\text{CIRh}(\text{CO})(\text{P}\sim\text{O})_2$ ($\text{O}\sim\text{P}$: $\eta^1\text{-P}$ -coordinated ether–phosphine ligand). One goal of the present work is to examine whether it is possible to combine the advantages of F–T/Q polymers¹⁶ (high degree of condensation and tuneable ratio of T/Q), with those of F–T/D blends (high flexibility and swelling ability). Moreover with the introduction of $\mathbf{1-D}^0\text{-C}_z\text{-D}^0$ we want to suppress the washing out of the D groups which we experienced with simple D groups such as $\text{Me}_2\text{Si}(\text{OEt})_2$.¹²

The most detailed information about the structure and mobility of these amorphous and insoluble materials is obtained by the multinuclear cross-polarization magic-angle spinning (CP/MAS) solid-state NMR spectroscopy.^{23–26} The phosphorus nucleus is an excellent probe to study supported phosphines and the geometry of their metal complexes. ¹³C CP/MAS NMR spectroscopy is used to establish the integrity of the spacers in the ligand and the methylene chains in the carbon backbone of the co-condensate. The structure

(21) Loy, D. A.; Carpenter, J. P.; Myers, S. A.; Assink, R. A.; Small, J. H.; Greaves, J.; Shea, K. J. *J. Am. Chem. Soc.* **1996**, *118*, 8501.

(22) Nomenclature of the compounds. *Integer*: type of reactive center (**1** = co-condensation agent, **2** = ligand, **3** = complex); *capital letter*: type of silicon species (**T** = three oxygen bonds, **D** = two oxygen bonds); *subscript*: stoichiometry of the silicon species; *superscript*: number of Si–O–Si bonds.

(23) Fyfe, C. A. *Solid State NMR for Chemists*; CRC Press: Guelph, ON, 1984.

(24) Engelhardt, G.; Michel, D. *High-resolution NMR of Silicates and Zeolites*; John Wiley and Sons: Chichester, 1987; p 106.

(25) Eckert, H. *Prog. Nucl. Magn. Reson. Spectrosc.* **1992**, *24*, 159.

(26) Schmidt-Rohr, K.; Spiess, H. W. *Multidimensional Solid State NMR and Polymers*; Academic Press: London, 1994.

(12) Lindner, E.; Schreiber, R.; Kemmler, M.; Schneller, T.; Mayer, H. A. *Chem. Mater.* **1995**, *7*, 951.

(13) Lindner, E.; Kemmler, M.; Schneller, T.; Mayer, H. A. *Inorg. Chem.* **1995**, *34*, 5489.

(14) Lindner, E.; Schreiber, R.; Schneller, T.; Wegner, P.; Mayer, H. A.; Göpel, W.; Ziegler, Ch. *Inorg. Chem.* **1996**, *35*, 514.

(15) Hagen, J. *Technische Katalyse*; VCH: Weinheim 1996.

(16) For the meaning of F–T/Q, F–T/T, and F–T/D blends: Copolymers prepared by simultaneous co-condensation of F–Si(OME)₃ with Si(OEt)₄ (**Q**⁰), MeSi(OME)₃ (**T**⁰) or Me₂Si(OEt)₂ (**D**⁰). F = PhP(CH₂CH₂OME)(CH₂)_z– and [cis-Cl(H)Ru(CO)]_{1/2}P(Ph)(CH₂CH₂OME)(CH₂)_z, respectively. **Q**: Q type silicon atom (four oxygen neighbors); **T**: T type silicon atom (three oxygen neighbors); **D**: D type silicon atom (two oxygen neighbors).

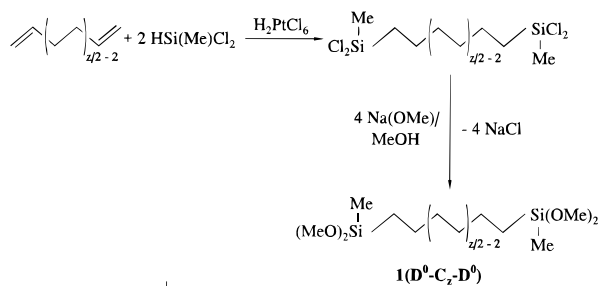
(17) Loy, D. A.; Shea, K. J. *Chem. Rev. (Washington, D.C.)* **1995**, *95*, 1431 and references therein.

(18) Corriu, R. J. P.; Moreau, J. J. E.; Thepot, P.; Wong Chi Man, M.; Choro, C. Lère-Porte, J.-P.; Sauvajol, J.-L. *Chem. Mater.* **1994**, *6*, 640.

(19) Loy, D. A.; Jamison, G. M.; Baugher, B. M.; Myers, S. A.; Assink, R. A.; Shea, K. J. *Chem. Mater.* **1996**, *8*, 656.

(20) Corriu, R.; Leclercq, D. *Angew. Chem., Int. Ed. Engl.* **1996**, *35*, 1420.

Scheme 2



z	monomeric co-condensation agents
6 (<i>n</i> -hexylene)	$1(D^0-C_6-D^0)$
8 (<i>n</i> -octylene)	$1(D^0-C_8-D^0)$
14 (<i>n</i> -tetradecylene)	$1(D^0-C_{14}-D^0)$

z = length of the $-CH_2-$ chain [z = 6, 8, 14]

D⁰: D type silicon atom (two oxygen neighbors)

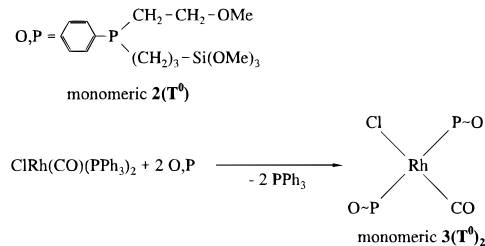
of the F–T/D–C_z–D matrixes is characterized by silicon-29 solid-state NMR spectroscopic studies. To get structural data of the atomic distances round the active metal center, EXAFS spectroscopical measurements are performed.

Results and Discussion

Preparation and Characterization of the Monomeric D- and T-Functionalized Precursors $1(D^0-C_z-D^0)$, $2(T^0)$, and $3(T^0)_2$.²² The bis(dimethoxymethylsilyl)alkanes $1(D^0-C_z-D^0)$ with *n*-hexylene, *n*-octylene, and *n*-tetradecylene bridges were prepared by hydrosilylation of the corresponding α,ω -alkadienes with dichloromethylsilane followed by methanolysis of the resulting α,ω -bis(dichloromethylsilyl)alkanes (Scheme 2). All monomers $1(D^0-C_z-D^0)$ were distilled under vacuum to afford clear, colorless and analytical pure liquids which dissolve readily in common organic solvents. The co-condensation agents $1(D^0-C_z-D^0)$ were completely characterized by ¹H, ¹³C{¹H}, and ²⁹Si{¹H} NMR, and mass spectroscopy (see Experimental Section).

The ether-phosphine ligand $2(T^0)$ (Scheme 3) was synthesized according to the literature.²⁷ This "hemilabile" ligand is able to form a close metal-phosphorus contact and only a weak metal-oxygen bond, that can dissociate from the metal in solution to provide free coordination sites in a catalytic cycle.²⁸ In addition $2(T^0)$ is equipped with a hydrolyzable trimethoxysilyl group. Substitution of triphenylphosphine in *trans*-ClRh(CO)(PPh₃)₂²⁹ with the more basic ether-phosphine $2(T^0)$ results in the generation of the yellow, monomeric complex $3(T^0)_2$. The ³¹P{¹H} NMR spectrum of $3(T^0)_2$ displays an A₂X pattern for the two equivalent phosphine ligands with a ¹J_{RhP} coupling constant consistent with the mutual trans positions of the phosphine ligands (see Experimental Section). The CO stretching frequency of $3(T^0)_2$ is also in agreement with the structure displayed in Scheme 3.^{30–32} The

Scheme 3



P–O: η^1 -P-coordinated ether-phosphine ligand PhP(CH₂CH₂OMe)(CH₂)₃Si(OMe)₃

T⁰: T type silicon atom (three oxygen neighbors)

square planar rhodium complex $3(T^0)_2$ was found to be stable under sol–gel reaction conditions as shown below.

Sol–Gel Processing. The properties of the products obtained by sol–gel polycondensations strongly depend on the reaction conditions such as concentration of the monomers, solvents, type of catalyst.⁹ The gelation of (EtO)₂MeSi(CH₂)₆SiMe(OEt)₂ occurs faster with NaOH than with HCl as catalyst, and the surface area of the acid-catalyzed polymer is lower than that of the basic catalyzed one.¹⁹ Since NaOH and HCl lead to decomposition of the monomeric ether-phosphine $2(T^0)$ and its corresponding rhodium(I) complex $3(T^0)_2$, in this and previous studies only (*n*-Bu)₂Sn(OAc)₂ was used as catalyst for all polycondensation reactions.^{1,12} Uniform reaction conditions were maintained for the hydrolysis, polycondensation, and co-condensation of the monomeric co-condensation agents $1(D^0-C_z-D^0)$, the monomeric ether-phosphine ligand $2(T^0)$, and its rhodium(I) complex $3(T^0)_2$ to achieve comparable results. Hence the components were mixed in the presence of (*n*-Bu)₂Sn(OAc)₂ with an excess of water. A minimum amount of alcohol was needed to homogenize the reaction mixtures.

According to this method three types of polysiloxanes (Scheme 4) were prepared. Type 1 is obtained by polycondensation of pure $1(D^0-C_z-D^0)$ to yield the corresponding polymer materials $1(D^I-C_z-D^I)$. Sol–gel processing of the T-functionalized ether-phosphine complex $3(T^0)_2$ without any co-condensation agent ($y = 0$; Scheme 4) leads to $3(T^0)_2$ (type 2). The F–T/D–C_z–D copolymers (type 3) were prepared by co-condensation of the monomers $2(T^0)$ and $3(T^0)_2$ with variable amounts of $1(D^0-C_z-D^0)$. The applied stoichiometries of the functionalized F–T⁰ groups and the co-condensation agents $1(D^0-C_z-D^0)$ were chosen in such a manner that the ratios of T:D in the resulting F–T/D–C_z–D copolymers are 1:2 ($y = 1$ and 2, respectively; Schemes 4 and 5). To investigate whether the ratio of T:D is tuneable in a wide range additional stoichiometries were employed in the co-condensation of $3(T^0)_2$ and $1(D^0-C_6-D^0)$ ($y = 1, 2, 4, 8, 16, 32$; Schemes 4 and 5). As a consequence of the normally incomplete condensation of all Si–OH groups, an excess of water has to be used in the sol–gel reactions of types 1–3 to achieve a high degree of hydrolysis. A comparison of the idealized and realistic composition (see below) of the polycondensation products is displayed in Scheme 5, and all prepared polysiloxanes are summarized in Table 1.

Solid-State NMR Spectroscopic Characterization of the Polymer Matrixes. Comparable stoichiometries and degrees of cross-linkage and of hydrolysis have to be ensured in order to investigate the influence of different lengths of the flexible bridging groups in the

(27) Lindner, E.; Bader, A.; Glaser, E.; Pfeleiderer, B.; Schumann, W.; Bayer, E. *J. Organomet. Chem.* **1988**, 355, 45.

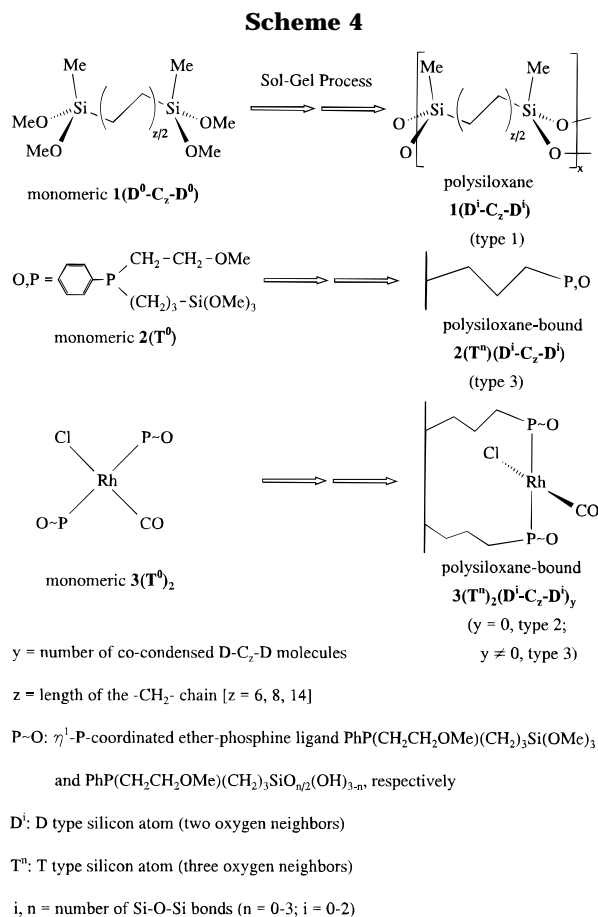
(28) Bader, A.; Lindner, E. *Coord. Chem. Rev.* **1991**, 108, 27.

(29) Evans, D.; Osborn, J. A.; Wilkinson, G. *Inorg. Synth.* **1968**, 11, 99.

(30) Lindner, E.; Wang, Q. Y.; Mayer, H. A.; Fawzi, R.; Steimann, M. *Organometallics* **1993**, 12, 1865.

(31) Brzezińska, Z. C.; Cullen, W. R. *Inorg. Chem.* **1979**, 18, 3132.

(32) Allum, K. G.; Hancock, R. D.; Howell, I. V.; McKenzie, S.; Pitkethly, R. C.; Robinson, P. J. *J. Organomet. Chem.* **1975**, 87, 203.



co-condensates $1(D^i-C_z-D^i)$ on the mobilities of the matrixes and the embedded ether phosphine ligands $2(T^n)(D^i-C_z-D^i)$ and corresponding complexes $3(T^n)_2(D^i-C_z-D^i)_y$.

²⁹Si CP/MAS NMR Spectroscopy. In the ²⁹Si CP/MAS NMR spectra signals of various substructures of the Dⁱ and Tⁿ units have been observed which indicate an incomplete condensation. The average chemical shifts are D⁰, -2.2; D¹, -13.6; D², -22.4; T¹, -52.3; T², -60.5; T³, -68.3.²² These chemical shifts are invariable with respect to the type of polysiloxane [$1(D^i-C_z-D^i)$, $3(T^n)_2$, and F-T/D-C_z-D] (Figures 1 and 2). The D and T groups are shifted to higher field with each increasing degree of condensation.²⁴

Small peaks at -5.4 ppm in the ¹³C CP/MAS NMR spectra of $1(D^i-C_z-D^i)$ are characteristic for the methyl groups bound to silicon atoms of the D⁰ groups. This is in contrast to the recently prepared hexylene bridged polysiloxane $1(D^i-C_6-D^i)$, in the spectra of which no D⁰ groups were detected.¹⁹ Those D⁰ species, which are attached to the polymer network via the second side of the bifunctional co-condensates, were not washed out during the solvent processing. It is assumed that the different sol-gel conditions are responsible for this result.³³

All types of silicon atoms in the polysiloxane matrixes $1(D^i-C_z-D^i)$, $2(T^n)(D^i-C_z-D^i)$, and $3(T^n)_2(D^i-C_z-D^i)_y$ have protons in distances that are close enough to get an efficient Hartmann-Hahn match.^{23,34} Therefore all silicon atoms are detectable with ²⁹Si CP/MAS NMR spectroscopy. The degree of condensation of the D and

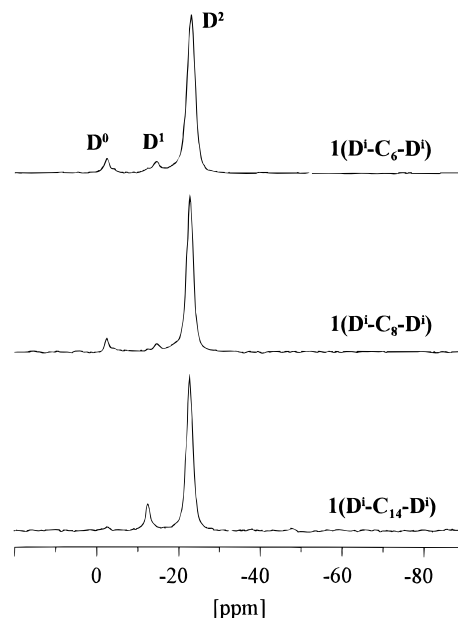


Figure 1. ²⁹Si CP/MAS NMR spectra of the polymers $1(D^i-C_z-D^i)$.

T species and the real ratios of D:T (Tables 2 and 3) were determined by generally known methods (see Experimental Section).³⁵⁻³⁷

Due to their ability to form four Si-O-Si linkages the polysiloxanes $1(D^i-C_z-D^i)$ can be regarded as "organofunctionalized Q analogues". Therefore they should build up highly cross-linked polysiloxane networks similar to those obtained by sol-gel processing of $\text{Si}(\text{OEt})_4$. For the series $1(D^i-C_z-D^i)$ higher degrees of condensation (91-99%)¹⁹ were obtained compared to a previously described silica gel (Q^k , 88%) which was prepared according to an analogous sol-gel route.¹⁰ The polymer $1(D^i-C_{14}-D^i)$ shows the highest degree of cross-linkage of the D groups (99%) of all obtained polysiloxanes (Tables 2 and 3). This is demonstrated in Figure 1, where $1(D^i-C_{14}-D^i)$ displays only a vanishing signal of the D⁰ species. It is concluded that the flexible methylene chain enables a nearly quantitative condensation.

In Figure 2 the ²⁹Si CP/MAS NMR spectra of the series of complexes $3(T^n)_2(D^i-C_6-D^i)_y$ ($y = 0, 1, 2, 4, 8, 16, 32$) are shown. It is recognizable that the ratio of T:D can be tuned which enables the control of the metal complex density within a F-T/D-C₆-D copolymer. The lowest degree of condensation of the T species (68%) in this series was found for $3(T^n)_2$ without any co-condensate ($y = 0$). Only slightly resolved signals were observed in the ²⁹Si CP/MAS NMR spectrum of $3(T^n)_2$ (Figure 2). The employment of small amounts ($y = 1$) of $1(D^0-C_6-D^0)$ in the sol-gel process of $3(T^n)_2$ leads to a higher degree of condensation of the T species and to a better resolved ²⁹Si CP/MAS NMR spectrum of the corresponding polysiloxane-bound complex $3(T^n)_2(D^i-C_6-D^i)$ (Figure 2). A further increase of the degree of condensation was achieved by adding more $1(D^0-$

(33) Khatib, I. S.; Parish, R. V. *J. Organomet. Chem.* **1989**, 369, 9.
 (34) Maciel, G. E.; Sindorf, D. W. *J. Am. Chem. Soc.* **1980**, 102, 7607.

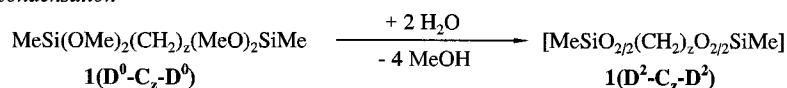
(35) The degree of condensation of the T species: $100(T^1 + 2T^2 + 3T^3)/[3(T^1 + T^2 + T^3)]$, degree of condensation of the D species: $100-(D^1 + 2D^2)/[2(D^0 + D^1 + D^2)]$; T¹, T², T³, D⁰, D¹, D² are the relative amounts of silyl species present in the sample (Tables 3 and 4).

(36) Mehring, M. *Principles of High Resolution NMR in Solids*, 2nd ed.; Springer-Verlag: Berlin, 1983.

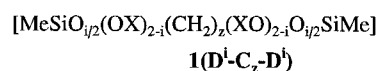
(37) Voelkel, R. *Angew. Chem., Int. Ed. Engl.* **1988**, 27, 1468.

Scheme 5

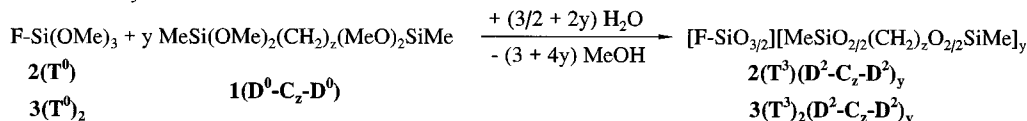
Idealized Polycondensation



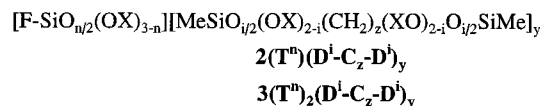
Realistic Composition of the Polycondensate:



Idealized Polycondensation



Realistic Composition of the Polycondensate:

F = PhP(CH₂CH₂OMe)CH₂CH₂CH₂- (2)F = [ClRh(CO)]_{1/2}P(Ph)(CH₂CH₂OMe)CH₂CH₂CH₂- (3)Tⁿ: T type silicon atom (three oxygen neighbors)Dⁱ: D type silicon atom (two oxygen neighbors)

i, n = number of Si-O-Si bonds

X = H, Me

y = amount of the co-condensate

z = length of the -CH₂- chain [z = 6, 8, 14]Table 1. Labeling of the Polymers and Copolymers²²

co-condensation agents	polymeric co-condensate	monomeric ligand 2(T⁰)	monomeric complex 3(T⁰)₂
1(D⁰-C₆-D⁰)	1(Dⁱ-C₆-Dⁱ)	2(Tⁿ)(Dⁱ-C₆-Dⁱ)	3(Tⁿ)₂ 3(Tⁿ)₂(Dⁱ-C₆-Dⁱ) 3(Tⁿ)₂(Dⁱ-C₆-Dⁱ)₂ 3(Tⁿ)₂(Dⁱ-C₆-Dⁱ)₄ 3(Tⁿ)₂(Dⁱ-C₆-Dⁱ)₈ 3(Tⁿ)₂(Dⁱ-C₆-Dⁱ)₁₆ 3(Tⁿ)₂(Dⁱ-C₆-Dⁱ)₃₂
1(D⁰-C₈-D⁰) 1(D⁰-C₁₄-D⁰)	1(Dⁱ-C₈-Dⁱ) 1(Dⁱ-C₁₄-Dⁱ)	2(Tⁿ)(Dⁱ-C₈-Dⁱ) 2(Tⁿ)(Dⁱ-C₁₄-Dⁱ)	3(Tⁿ)₂(Dⁱ-C₈-Dⁱ)₂ 3(Tⁿ)₂(Dⁱ-C₁₄-Dⁱ)₂

C₆-D⁰) ($y = 2, 4, 8, 16, 32$) to **3(T⁰)₂**. Up to a ratio of T:D = 1:4 the degree of condensation of the T groups is approximately constant in the range of 90–91% indicating an upper limit. For the degree of condensation of the D groups in the series **3(Tⁿ)₂(Dⁱ-C₆-Dⁱ)_y** ($y = 1, 2, 4, 8, 16, 32$) a similar trend was found (Table 3). The bulky complex obviously prevents a complete condensation of the hydroxyl groups. It is deduced from the ²⁹Si CP/MAS NMR spectra, that the degree of condensation of the T groups is not affected by the length of the flexible bridging groups. This is in contrast to the degree of condensation of the D groups. The tetradecylene chain in the D-C₁₄-D and F-T/D-C₁₄-D polycondensates obviously enables a better orientation of the SiOH groups to each other. Thus a higher degree of condensation is achieved.

¹³C CP/MAS NMR Spectroscopy. In the ¹³C CP/MAS NMR spectra of the co-condensates **1(Dⁱ-C_z-Dⁱ)** three [**1(Dⁱ-C₆-Dⁱ)**]¹⁹ and four [**1(Dⁱ-C₈-Dⁱ)** and **1(Dⁱ-C₁₄-Dⁱ)**] types of resonances for the bridging methylene carbon atoms were observed. All polymers **1(Dⁱ-C_z-Dⁱ)** display one resonance at 18 ppm assigned to the carbon atoms directly bound to the silicon atoms and two resonances at 23.3 and 33.6 ppm due to the carbon nuclei in the β and γ position of the hydrocarbon bridges.

A further signal at 30.1 ppm is observed in the spectra of **1(Dⁱ-C₈-Dⁱ)** and **1(Dⁱ-C₁₄-Dⁱ)** caused by the remaining carbon atoms of the flexible bridging groups. The carbon nuclei of the methyl groups attached to the single and 2-fold condensed silicon atoms (D¹ and D²) of all polymers **1(Dⁱ-C_z-Dⁱ)** give rise to a single peak at 0 ppm. The low-field shift (~5 ppm) with respect to the monomeric congeners of the signals of the carbon nuclei directly bound to the silicon atoms is in agreement with the formation of Si-O-Si bonds.

Mainly four groups of signals are distinguished in the ¹³C CP/MAS NMR spectra of the supported ligands **2-(Tⁿ)(Dⁱ-C_z-Dⁱ)** and complexes **3(Tⁿ)₂(Dⁱ-C_z-Dⁱ)_y** (see Table 1): The carbon nuclei of the phenyl groups in the aromatic region between 139.2 and 128.4, those adjacent to the ether oxygen atoms [CH₂O (70.3–67.7 ppm) and OCH₃ (58.4–57.9 ppm)], a complex pattern due to the methylene groups in the region between 40 and 10 ppm, and with exception of **3(Tⁿ)₂** one resonance for the SiCH₃ groups at 0.3 to -0.2 ppm (D¹ and D²). All polymers and copolymers reveal an additional small peak at 49.5–50.2 ppm in the ¹³C CP/MAS NMR spectra which is attributed to residual methoxy substituents. Hence the degree of hydrolysis of all these samples range between 91 and 99% (see Tables 2 and 3).³⁸ Not

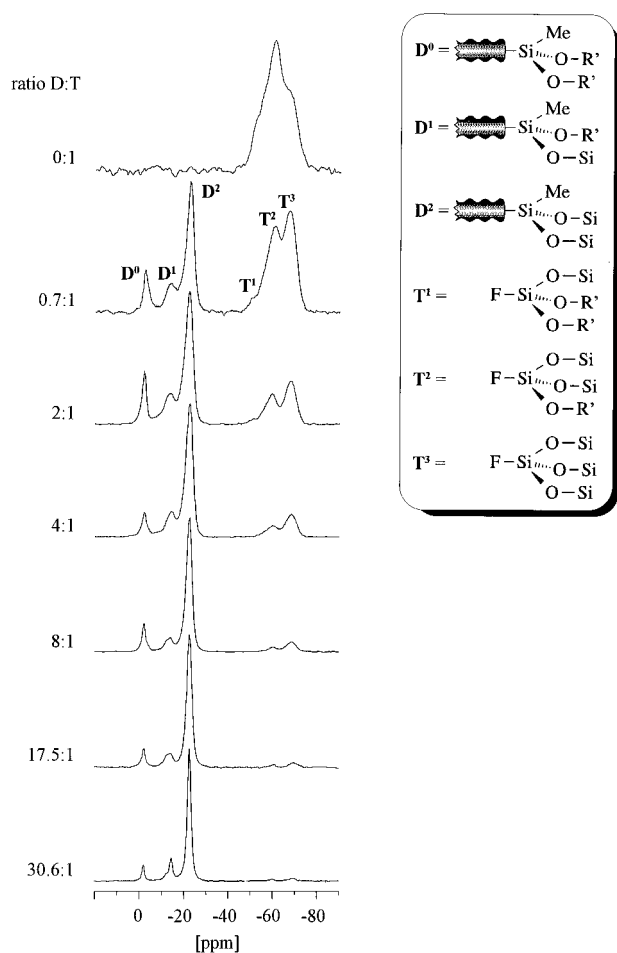


Figure 2. ^{29}Si CP/MAS NMR spectra of the copolymers $3(\text{T}^n)(\text{D}^i-\text{C}_z-\text{D}^j)_y$. The various silyl species are schematically displayed.

all SiOCH_3 bonds seem to be accessible to the water molecules, due to the hydrophobic character of the matrix.

It is resumed from the solid-state NMR spectroscopic studies of the matrixes that the T:D ratios are in good agreement with the stoichiometries applied in the sol-gel process. With exception of $3(\text{T}^n)_2$ all polycondensates show high degrees of condensation (Tables 2 and 3). Moreover the ^{13}C CP/MAS NMR spectra of all components give evidence for intact silicon-carbon and phosphorus-carbon bonds of the co-condensates and the ligands.³⁹

^{31}P CP/MAS NMR and IR Spectroscopic Characterization of the Reactive Centers. The IR and ^{31}P CP/MAS NMR spectra of $2(\text{T}^n)(\text{D}^i-\text{C}_z-\text{D}^j)$ and $3(\text{T}^n)_2(\text{D}^i-\text{C}_z-\text{D}^j)_y$ confirm that the ligands and the geometry of the complex *trans*-ClRh(CO)(P~O)₂ are

(38) The degree of hydrolysis of the D species in the $\text{D}-\text{C}_z-\text{D}$ polymers is calculated by the following equation: $100[2 - A(\text{Si}-\text{OCH}_3)/A(\text{Si}-\text{CH}_3)]/2$; $A(\text{Si}-\text{OCH}_3)$ = peak area of the nonhydrolyzed $\text{Si}-\text{O}-\text{CH}_3$ group in the ^{13}C CP/MAS NMR spectrum; $A(\text{Si}-\text{CH}_3)$ = peak area of the methyl group in the ^{13}C CP/MAS NMR spectrum. The overall degree of hydrolysis of the D and T species in the F-T/D-C_z-D copolymers is calculated by the following equation: $100[(3T + 2D) - A(\text{Si}-\text{OCH}_3)/A(\text{CH}_2-\text{O}-\text{CH}_3)]/(3T + 2D)$; T = real amount of T species in the polymer; D = real amount of D species in the polymer (see Table 3); $A(\text{Si}-\text{OCH}_3)$ = peak area of the nonhydrolyzed $\text{Si}-\text{O}-\text{CH}_3$ group in the ^{13}C CP/MAS NMR spectrum; $A(\text{CH}_2-\text{O}-\text{CH}_3)$ = peak area of the methoxy group in the ^{13}C CP/MAS NMR spectrum.

(39) A more detailed description of the network architecture of these materials as outlined above, especially whether cycles are formed,²¹ is not possible.

preserved during the sol-gel reaction. Thus the polysiloxane-bound ether-phosphine ligands $2(\text{T}^n)(\text{D}^i-\text{C}_z-\text{D}^j)$ give rise to one signal in the ^{31}P CP/MAS NMR spectra at -32 ppm (Figure 3) which is in accordance with the monomeric precursor $2(\text{T}^0)$ in solution.⁴⁰ No phosphine oxide species are present in the spectra of $2(\text{T}^n)(\text{D}^i-\text{C}_z-\text{D}^j)$.^{8,41} In the ^{31}P CP/MAS NMR spectra of the immobilized rhodium(I) complexes $3(\text{T}^n)_2(\text{D}^i-\text{C}_z-\text{D}^j)_y$ only one resonance flanked by spinning sidebands has been observed (Table 4, Figure 4). The chemical shifts of $3(\text{T}^n)_2(\text{D}^i-\text{C}_z-\text{D}^j)_y$ (Table 4) are compatible to that of the monomeric counterpart $3(\text{T}^0)_2$ (see Experimental Section). The enhanced dispersion of the chemical shifts of the phosphorus nuclei increases the line width of the signals in the solid state. Therefore the coupling between rhodium and phosphorus is not resolved. The position of the $\text{C}=\text{O}$ absorption band in the carbonyl region of the IR spectra of the rhodium functionalized polymers is comparable to that of the monomeric congener $3(\text{T}^0)_2$ in solution (see Experimental Section).

EXAFS Spectroscopic Characterization of $3(\text{T}^n)_2$.

The amorphous character of the stationary phases makes it impossible to get structural data about the polysiloxane-bound complexes with conventional X-ray diffraction. The properties of EXAFS spectroscopy, however, allows the determination of the local structure round the rhodium atom, independent of the sample's physical state. The measurements were carried out on $3(\text{T}^n)_2$, because this sample has the greatest rhodium content of all. The experimental EXAFS function can be described with at least three shells. The assumption of one chlorine atom, two equivalent phosphorus atoms and one carbon atom leads to a good agreement between the experimental and the calculated functions. A remarkable improvement can be obtained if an additional oxygen atom is assumed in the simulation (see Table 5). But this atom, which belongs to the linear carbonyl ligand, makes it necessary to perform complex multiple scattering calculations. Only in this way the EXAFS function can be described completely. The influence of multiple scattering in the Fourier transform is shown in Figure 5.

The obtained two equal phosphorus distances are a confirmation of the ^{31}P CP/MAS NMR experiments, from which a *trans* position of the phosphine ligands can be deduced. A really interesting result is the distance of the carbonyl ligand of 1.77 Å, which is very short. But the corresponding Rh-O distance, which is also shorter than in most cases, confirms that in fact the carbonyl group is very close to the metal center. Anyway, the indirectly obtained C-O distance of 1.16 Å is in a range acceptable for carbonyl ligands.

Studies on the Dynamic Behavior of the Polysiloxanes by ^{29}Si , ^{31}P CP/MAS NMR, and 2D WISE NMR Spectroscopy. To optimize the stationary component for the employment in interphase reactions, it is necessary to get detailed knowledge of the dynamic properties of the matrixes and the reactive centers. Enhanced mobilities should result in a better uniformity and accessibility of the reactive centers and thus in higher activities and selectivities in catalytic reactions.

(40) Lindner, E.; Kemmler, M.; Mayer, H. A. *Chem. Ber.* **1992**, 125, 2385.

(41) Blümel, J. *GIT Fachz. Lab.* **1994**, 5, 510.

Table 2. Relative I_0 , T_{SiH} , $T_{1\rho H}$, and T_{1Si} Data of the Silyl Species in the D-C_z-D Polymers

compound	relative I_0 data ^a			degree of condensation [%]	degree of hydrolysis [%] ^b	T_{SiH} [ms] ^c			$T_{1\rho H}$ [ms] ^d	T_{1Si} [s] ^e		$\nu_{1/2}$ [Hz]	
	D ⁰	D ¹	D ²			D ⁰	D ¹	D ²		D ¹	D ²	D ¹	D ²
1(Dⁱ-C₆-D^j)	5.8	5.9	100	92	99	2.16	1.00	1.28	4.5	10.6	14.4	82	93
1(Dⁱ-C₈-D^j)	5.9	3.6	100	93	96	2.40	1.34	1.02	3.2	14.1	14.4	86	92
1(Dⁱ-C₁₄-D^j)	0.1	1.3	100	99	97	<i>f</i>	1.68	0.96	3.0	<i>f</i>	9.7	62	73

^a I_0 values are calculated from eq 1 (see Experimental Section). ^b For the determination of the degree of hydrolysis see ref 38. ^c Determined by contact time variation. ^d Determined via ²⁹Si with the experiment according to Schaefer (see Experimental Section). ^e Values from the experiment according to Torchia (see Experimental Section). ^f Intensity too low for a precise determination of T_{SiH} and T_{1Si} .

Table 3. Relative I_0 , T_{SiH} , and $T_{1\rho H}$ Data of the Silyl Species in the F-T/D-C_z-D Copolymers

compound	relative I_0 data of D and T species ^a						degree of condensation [%]		real T/D moiety	degree of hydrolysis [%] ^b	T_{SiH} [ms] ^c					$T_{1\rho H}$ [ms] ^d
	D ⁰	D ¹	D ²	T ¹	T ²	T ³	D	T			D ⁰	D ¹	D ²	T ²	T ³	
2(Tⁿ)(Dⁱ-C₆-D^j)	6.7	16.0	100	<i>e</i>	15.5	44.3	88	91	1:2.1	93	<i>f</i>	<i>f</i>	0.88	<i>f</i>	0.59	2.1
2(Tⁿ)(Dⁱ-C₈-D^j)	2.9	11.2	100	<i>e</i>	13.8	40.4	93	92	1:2.1	96	<i>f</i>	<i>f</i>	1.09	<i>f</i>	0.79	2.5
2(Tⁿ)(Dⁱ-C₁₄-D^j)	<i>e</i>	8.5	100	<i>e</i>	22.6	36.1	96	87	1:1.9	91	<i>e</i>	<i>f</i>	0.88	<i>f</i>	0.82	2.0
3(Tⁿ)₂				72.9	100	81.7		68	1:0	98				0.97	0.96	5.7
3(Tⁿ)₂(Dⁱ-C₆-D^j)	22.2	27.9	98.4	29.2	99.0	100	75	77	1:0.7	96	1.67	1.03	1.28	1.13	1.33	6.5
3(Tⁿ)₂(Dⁱ-C₆-D^j)₂	25.3	39.1	100	6.5	30.9	45.1	73	82	1:2	91	2.35	1.22	1.46	1.14	1.5	5.5
3(Tⁿ)₂(Dⁱ-C₆-D^j)₄	12.1	20.8	100	<i>e</i>	9.2	23.9	83	91	1:4	96	2.34	1.17	1.62	1.08	1.23	6.7
3(Tⁿ)₂(Dⁱ-C₆-D^j)₈	15.8	14.1	100	<i>e</i>	4.5	11.7	82	91	1:8	94	2.92	1.21	1.46	1.16	1.08	6.5
3(Tⁿ)₂(Dⁱ-C₆-D^j)₁₆	10.5	14.5	100	<i>e</i>	2.2	4.9	86	90	1:17.5	92	2.24	1.13	1.36	0.88	0.91	8.8
3(Tⁿ)₂(Dⁱ-C₆-D^j)₃₂	9.2	16.2	100	<i>e</i>	1.1	3.1	86	91	1:30.6	93	2.01	0.97	0.92	<i>f</i>	<i>f</i>	5.8
3(Tⁿ)₂(Dⁱ-C₈-D^j)₂	18.6	38.5	100	3.9	36.3	42.1	76	82	1:1.9	91	1.91	0.88	1.11	1.17	1.18	4.9
3(Tⁿ)₂(Dⁱ-C₁₄-D^j)₂	8.0	24.1	100	0.1	31.3	37.2	85	85	1:1.9	96	2.08	1.42	1.62	1.41	1.68	4.8

^a I_0 values calculated from eq 1 (see Experimental Section). ^b For the determination of the degree of hydrolysis see ref 38. ^c Determined by contact time variation. ^d Determined via ²⁹Si with the experiment according to Schaefer (see Experimental Section). ^e Species not detectable. ^f Intensity too low for a precise determination of T_{SiH} .

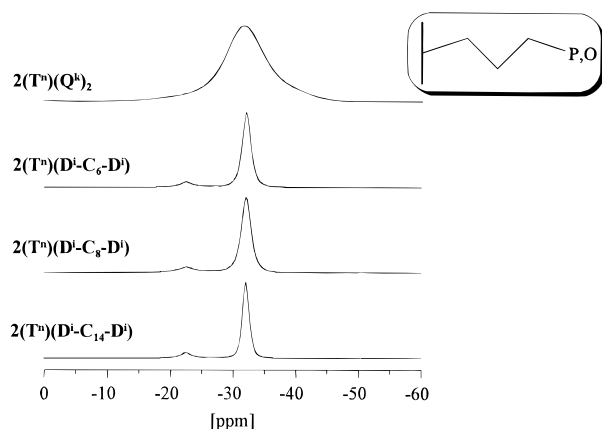


Figure 3. ³¹P CP/MAS NMR spectra of the polysiloxane-bound ether-phosphine ligands **2(Tⁿ)(Q^k)₂** and **2(Tⁿ)(Dⁱ-C_z-D^j)** ($\nu_{rf} = 5$ kHz).

A number of NMR parameters such as T_{1X} , T_{XH} ($X = {}^{13}\text{C}$, ²⁹Si, ³¹P), $T_{1\rho H}$, and the line width of the heteronuclei X in the corresponding CP/MAS NMR spectra are sensitive toward motions on different time scales.

Motions in the MHz region are responsible for the spin-lattice relaxation times T_{1X} which are characteristic for individual nuclei. If enhanced mobilities in the kHz region reduce the dipolar coupling among the protons, different spin-lattice relaxation time constants of the protons in the rotating frame $T_{1\rho H}$ for certain parts of the material can be obtained.^{42,43} The $T_{1\rho H}$ relaxation time is an averaged quantity for all protons within domains of 1–2 nm in diameter in those cases where an efficient spin diffusion process is present. An unambiguous discussion of the dynamic properties of

Table 4. ³¹P CP/MAS, T_{PH} , $T_{1\rho H}$, and T_{1P} Data of the Polysiloxane-Bound Ether-Phosphine Ligand **2 and the Complex **3** with Different Co-condensates**

compound	δ ³¹ P [ppm]	T_{PH} [ms] ^a	$T_{1\rho H}$ [ms] ^b	$\nu_{1/2}$ [Hz]	T_{1P} [s] ^c
2(Tⁿ)(Q^k)₂^d	-31.7	0.29	1.4	900	7.0
2(Tⁿ)(Dⁱ-C₆-D^j)	-32.0	0.64	2.0	197	3.6
2(Tⁿ)(Dⁱ-C₈-D^j)	-32.0	0.56	2.1	224	3.8
2(Tⁿ)(Dⁱ-C₁₄-D^j)	-31.9	0.91	2.1	156	2.0
3(Tⁿ)₂	15.5	0.26	4.2	1669	11.8
3(Tⁿ)₂(Dⁱ-C₆-D^j)	16.0	0.26	4.7	1561	11.4
3(Tⁿ)₂(Dⁱ-C₆-D^j)₂	16.2	0.22	5.4	1450	10.3
3(Tⁿ)₂(Dⁱ-C₆-D^j)₄	16.5	0.27	5.1	1360	8.6
3(Tⁿ)₂(Dⁱ-C₆-D^j)₈	16.4	0.27	4.8	1203	7.8
3(Tⁿ)₂(Dⁱ-C₆-D^j)₁₆	16.0	0.25	5.6	1200	7.1
3(Tⁿ)₂(Dⁱ-C₆-D^j)₃₂	16.6	0.27	4.0	918	6.2
3(Tⁿ)₂(Dⁱ-C₈-D^j)₂	16.4	0.23	4.3	1390	9.5
3(Tⁿ)₂(Dⁱ-C₁₄-D^j)₂	16.3	0.25	2.7	1232	9.1

^a Determined by contact time variation. ^b Determined via ³¹P with the experiment according to Schaefer (see Experimental Section). ^c Values from the NMR experiment according to Torchia (see Experimental Section) at 294 K. ^d **2(Tⁿ)** reacted with Si(OEt)₄ (Q⁰) ($k = 0-4$, number of Si-O-Si bonds); see refs 2 and 10.

different materials on the basis of these relaxation parameters is only possible, if the corresponding correlation time τ_c is considered. The dependence of T_{1X} and $T_{1\rho H}$ on the correlation time τ_c is given by the correlation time curve.²³ Temperature-dependent relaxation time measurements are able to distinguish between two cases. In the slow motion regime decreasing relaxation times correlate with decreasing τ_c (increasing temperature) and thus faster motions, whereas in the fast-motion regime the relaxation times are increasing with faster motions (shorter τ_c). The number of protons and their distances from the heteronuclei and the rigidity of the heteronuclear coupled spin systems (phosphorus and protons, e.g.) influence the cross polarization constants T_{XH} . If the number and distances of the protons surrounding the corresponding nuclei in different compounds is equal or very similar the T_{XH}

(42) Schaefer, J.; Stejskal, E. O.; Buchdahl, R. *Macromolecules* **1977**, *10*, 384.

(43) Koenig, J. L.; Andreis, M. *Solid State NMR of Polymers*; Mathias, L. J., Ed.; Plenum Press: New York, 1991; p 201.

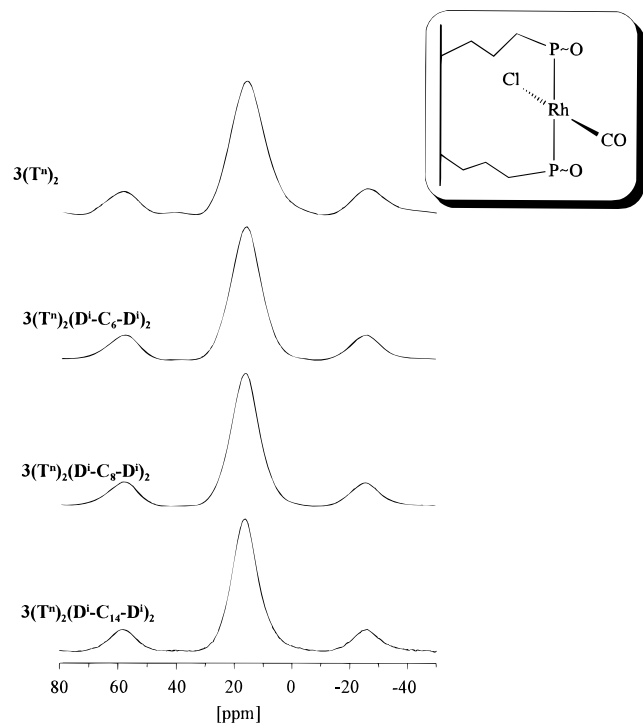


Figure 4. ^{31}P CP/MAS NMR spectra of the polysiloxane-bound rhodium(I) complexes $3(\text{T}^n)_2(\text{D}^i-\text{C}_z-\text{D}^j)_y$ ($\nu_{\text{rf}} = 5$ kHz).

Table 5. EXAFS Spectroscopical Determined Structural Data Absorber-Backscatterer Distance [Å], Coordination Number, and Debye-Waller Factor σ [Å] of $3(\text{T}^n)_2$ (Errors of r and N Given in Parentheses)

	r [Å]	N	σ [Å]
Rh-C	1.77 (± 0.01)	1 (± 0.15)	0.084
Rh-P	2.23 (± 0.02)	2 (± 0.20)	0.089
Rh-Cl	2.32 (± 0.02)	1 (± 0.20)	0.055
Rh-O	2.93 (± 0.01)	1 (± 0.15)	0.077

constants are solely determined by their mobilities. Thus faster motions lead to an inefficient magnetization transfer of the protons to the X atoms and therefore to higher T_{XH} values.

Several interactions such as heteronuclear dipolar coupling, chemical shift anisotropy (CSA), and chemical shift dispersion contribute to the line widths of the X atoms in the solid-state NMR spectra.^{23,24} Since the local environments of the silicon and phosphorus atoms in the D-C_z-D polymers, ligands, and complexes of the different copolymers are very similar the changes of the line widths of the ^{29}Si and ^{31}P signals in the corresponding CP/MAS NMR spectra are caused by the variable flexibilities of the materials.

Mobilities of the Matrixes. The $T_{1\rho\text{H}}$ (via ^{29}Si), and $T_{1\text{Si}}$ values, as well as the half line widths are depicted in Table 2. Silica gels show much higher $T_{1\rho\text{H}}$ values (typically 20–50 ms^{10,34,44}) than those reported for organofunctionalized analogues $1(\text{D}^i-\text{C}_z-\text{D}^j)$ in this work (Table 2). Temperature-dependent studies demonstrate that the $T_{1\rho\text{H}}$ relaxation times (via ^{29}Si) of $1(\text{D}^i-\text{C}_6-\text{D}^j)$ [294 K: 4.5 ms; 313 K: 11.2 ms; 333 K: 14.1 ms; 353 K: 18.8 ms] increase with increasing temperature. Thus higher $T_{1\rho\text{H}}$ values correspond to shorter correlation times τ_c and therefore to higher mobilities in the kHz region.²³ An analogous tendency

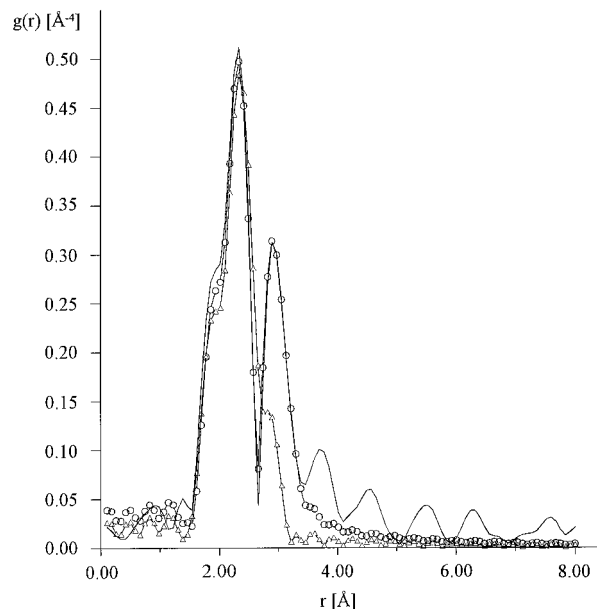


Figure 5. Fourier transforms of $3(\text{T}^n)_2$: Experimental, calculated (triangle), and with multiple scattering calculated (circle) functions.

was found for the spin lattice relaxation time $T_{1\text{Si}}$ of the D² groups in $1(\text{D}^i-\text{C}_6-\text{D}^j)$ at different temperatures [294 K: 14.4 s; 313 K: 17.1 s; 333 K: 20.5 s; 353 K: 30.0 s]. The polycondensate $1(\text{D}^i-\text{C}_{14}-\text{D}^j)$ reveals narrower lines in the ^{29}Si CP/MAS NMR spectrum than $1(\text{D}^i-\text{C}_6-\text{D}^j)$ and $1(\text{D}^i-\text{C}_8-\text{D}^j)$ (Figure 1) indicating a higher flexibility of this polymer network compared to $1(\text{D}^i-\text{C}_6-\text{D}^j)$ and $1(\text{D}^i-\text{C}_8-\text{D}^j)$.

The methyl groups of the D units contribute to the relaxation of the silicon atoms in the MHz region, due to their fast rotation.^{45,46} This is also confirmed by the higher cross polarization constant ($T_{\text{CH}} = 850$ μs) of the methyl groups attached to the silicon atoms relative to those of the methylene carbon atoms in the hexylene bridge ($T_{\text{CH}} = 660$ – 720 μs ; see Experimental Section). The fast methyl group rotation leads to shorter $T_{1\text{Si}}$ values for the Dⁱ units than for the Tⁿ units in the case of $3(\text{T}^n)_2(\text{D}^i-\text{C}_6-\text{D}^j)_2$ [$T_{1\text{Si}}(\text{D}^2)$: 18.0 s, $T_{1\text{Si}}(\text{T}^3)$: 55.7 s, e.g., see Experimental Section]. In the series of the co-condensed complexes $3(\text{T}^n)_2(\text{D}^i-\text{C}_z-\text{D}^j)_y$, no significant differences in the dynamic parameters (Table 3) between various samples [$T_{1\text{SiH}}$, $T_{1\rho\text{H}}$ (via ^{29}Si)] were observed. Therefore no conclusions about the mobilities of these silicon matrixes can be drawn.

Mobilities of the Reactive Centers. In recent works it was demonstrated that the phosphorus atom in the ligand $2(\text{T}^n)$ is an excellent tool to study the influence of different matrixes on the dynamic behavior of the co-condensed reactive centers.^{2,10,12} In Figure 3 the ^{31}P CP/MAS NMR spectra of the polysiloxane-bound ligands $2(\text{T}^n)(\text{D}^i-\text{C}_z-\text{D}^j)$ and $2(\text{T}^n)(\text{Q}^k)_2$ with different co-condensates are displayed. The line widths of the ^{31}P CP/MAS NMR signals of $2(\text{T}^n)(\text{D}^i-\text{C}_z-\text{D}^j)$ are remarkably reduced with respect to their Q analogue $2(\text{T}^n)(\text{Q}^k)_2$ (Table 4, Figure 3). Simultaneously an increase of the T_{PH} constants from 0.29 to 0.91 in the sequence $2(\text{T}^n)(\text{Q}^k)_2 < 2(\text{T}^n)(\text{D}^i-\text{C}_6-\text{D}^j) \approx 2(\text{T}^n)(\text{D}^i-\text{C}_8-\text{D}^j) <$

(45) Alemany, L. B.; Grant, D. M.; Pugmire, R. J.; Alger, T. D.; Zilm, K. W. *J. Am. Chem. Soc.* **1983**, *105*, 2133.

(46) Alemany, L. B.; Grant, D. M.; Pugmire, R. J.; Alger, T. D.; Zilm, K. W. *J. Am. Chem. Soc.* **1983**, *105*, 2143.

(44) Pfeleiderer, B.; Albert, K.; Bayer, E.; van den Ven, L. de Haan, J.; Cramers, C. *J. Phys. Chem.* **1990**, *94*, 4189.

Table 6. Temperature-Dependent $T_{1\rho\text{H}}$ and $T_{1\text{P}}$ Relaxation Times of the Polysiloxane-Bound Ether–Phosphine **2 with Different Co-condensates and the Complex **3**(T^n)₂($\text{D}^i\text{-C}_6\text{-D}^j$)₂**

compound	$T_{1\rho\text{H}}$ [ms] ^a					$T_{1\text{P}}$ [s] ^b				
	294 K	313 K	323 K	333 K	348 K	294 K	313 K	323 K	333 K	348 K
2 (T^n)($\text{D}^i\text{-C}_6\text{-D}^j$)	2.0	3.7	5.0	6.6		3.6	3.4	3.1	3.1	
2 (T^n)($\text{D}^i\text{-C}_8\text{-D}^j$)	2.1	3.0	4.1	7.5		3.8	3.1	2.9	3.3	
2 (T^n)($\text{D}^i\text{-C}_{14}\text{-D}^j$)	2.1	4.3	5.0	6.3		2.0	2.9	3.1	3.2	
3 (T^n) ₂ ($\text{D}^i\text{-C}_6\text{-D}^j$) ₂	5.4	5.2		4.5	3.9	10.3	8.6		7.7	6.8

^a Determined via ³¹P with the experiment according to Schaefer (see Experimental Section). ^b Values from the NMR experiment according to Torchia (see Experimental Section).

2(T^n)($\text{D}^i\text{-C}_{14}\text{-D}^j$) is observed, indicating higher mobilities of the phosphorus atoms in these F–T/D–C_z–D co-condensates (Scheme 1). The extension of *z* from 6 via 8 to 14 in **2**(T^n)($\text{D}^i\text{-C}_z\text{-D}^j$) results in the slowest magnetization of the phosphorus atom (longest T_{PH} constant), the smallest line width (156 Hz), and the fastest spin–lattice relaxation ($T_{1\text{P}} = 2.0$ s) in the series of the co-condensed ligands. This is consistent with the conclusion that **2**(T^n)($\text{D}^i\text{-C}_{14}\text{-D}^j$) is the most flexible ligand in these F–T/D–C_z–D copolymers. From a temperature-dependent study it is known that the $T_{1\text{P}}$ values of **2**(T^n)(Q^k)₂ decrease with increasing temperature.¹⁰ Thus shorter $T_{1\text{P}}$ times correspond to shorter correlation times τ_c and therefore to higher mobilities in the MHz region.²³ A similar tendency was found for **2**(T^n)($\text{D}^i\text{-C}_6\text{-D}^j$) and **2**(T^n)($\text{D}^i\text{-C}_8\text{-D}^j$) (Table 6), whereas $T_{1\text{P}}$ of the highly mobile ligand **2**(T^n)($\text{D}^i\text{-C}_{14}\text{-D}^j$) is already in the extreme narrowing limit since $T_{1\text{P}}$ changes from 2.0 s (294 K) via 2.9 s (313 K) to 3.1 s (323 K) and 3.2 s (333 K). Moreover the $T_{1\rho\text{H}}$ relaxation times of the F–T/D–C_z–D co-condensates are located in the fast-motion regime of the correlation time curve (Table 6) pointing to the enhanced flexibilities of these materials.

The coordination of three ether–phosphines in the octahedral ruthenium(II) complex *cis*-H(Cl)Ru(CO)(P~O)₃ leads to an additional cross-linkage of the matrixes via the metal center and therefore to a strong reduction of the mobilities of the corresponding phosphorus atoms. As a consequence the differences in the dynamic parameters between different materials are not as significant as those observed in the immobilized ligands.^{2,10,12} In continuation of our investigations we were now also interested in the influence of the two ether–phosphine ligands in the square planar rhodium(I) complex ClRh(CO)(P~O)₂ on these dynamic parameters (Scheme 3). The T_{PH} values of all compounds **3**(T^n)₂($\text{D}^i\text{-C}_z\text{-D}^j$)₂ drop close to 0.25 ms (Scheme 4, Table 4) which is in the same range as for the above-mentioned ruthenium(II) complex ($T_{\text{PH}} = 0.2$ ms). The P coordination enables a fast polarization transfer for all types of D–C_z–D co-condensates even in the case when only two ligands are bound to one rhodium center. This is due to the higher rigidity of the phosphorus atom of the coordinated ligand. Compared to the ligands **2**(T^n)($\text{D}^i\text{-C}_z\text{-D}^j$), longer $T_{1\text{P}}$ values of the polysiloxane-bound complexes **3**(T^n)₂($\text{D}^i\text{-C}_z\text{-D}^j$)₂ (Table 4) also emphasize the reduced mobility caused by the anchoring of the ligands to the metal center. Temperature-dependent measurements of $T_{1\rho\text{H}}$ (via ³¹P) on **3**(T^n)₂($\text{D}^i\text{-C}_6\text{-D}^j$)₂ show decreasing relaxation times on going from ambient temperature to higher temperatures (Table 6), indicating strong dipolar interactions of the protons at ambient temperature. Thus conclusions about segmental mobilities cannot be drawn from this

parameter.^{47,48} Decreasing line widths of the ³¹P resonances of the immobilized complexes **3**(T^n)₂($\text{D}^i\text{-C}_z\text{-D}^j$)₂ dependent on the length of the flexible bridging groups (hexylene ≈ octylene > tetradecylene, see Table 4 and Figure 4), again confirm the highest mobility for the F–T/D–C₁₄–D copolymer in this series. This observation is accompanied by the lowest $T_{1\rho\text{H}}$ (via ³¹P) and $T_{1\text{P}}$ values for **3**(T^n)₂($\text{D}^i\text{-C}_{14}\text{-D}^j$)₂ (Table 4).

The line widths of the ³¹P signals of the copolymerized rhodium complexes **3**(T^n)₂($\text{D}^i\text{-C}_6\text{-D}^j$)₂ also depend on the number (*y*) of the added co-condensate D–C₆–D. Narrower lines were observed for increasing amounts of the co-condensate (Table 4). In addition a continuous decrease of the $T_{1\text{P}}$ constants in the same sequence from 11.8 s (*z* = 0) to 6.2 s (*z* = 32) was determined. Both sets of data point to higher mobilities of the phosphorus atoms in the MHz region if more D–C₆–D is employed in these materials. Enhanced temperatures in the case of **3**(T^n)₂($\text{D}^i\text{-C}_6\text{-D}^j$)₂ also result in a continuous reduction of the line widths of the ³¹P resonances from 1450 Hz (294 K) to 1048 Hz (348 K) (see Experimental Section). Simultaneously the $T_{1\text{P}}$ relaxation times decrease (Table 6). From these aforementioned observations it is concluded that either the employment of more D–C₆–D co-condensation agent or rising temperatures lead to enhanced dynamic properties of the F–T/D–C₆–D copolymers.

2D WISE NMR Spectroscopy. To get a correlation between the segmental mobility and the chemical structure and therefore a more detailed knowledge about the mobilities of different parts of the copolymers the two-dimensional heteronuclear wide-line separation (WISE) spectroscopy was applied. The pulse sequence of the WISE experiment starts with a ¹H 90° pulse followed by an incremented proton evolution time (*t*₁) after which the proton magnetization is transferred to ¹³C via the Hartmann–Hahn cross polarization, i.e., 90° (¹H)–*t*₁–CP acquisition.⁴⁹ Slices at individual ¹³C resonances in a 2D data set reveal the ¹H line widths of the various structural moieties within a sample. The line widths in the F1 (proton) dimension are determined by ¹H–¹H dipolar interactions, which are reduced by molecular motion and magic angle spinning. In Figure 6 the WISE spectrum of the polysiloxane-bound ligand **2**(T^n)($\text{D}^i\text{-C}_6\text{-D}^j$) is displayed. The corresponding structural elements are also shown in this figure. From the ³¹P relaxation time studies of the co-condensed ligand **2**(T^n)($\text{D}^i\text{-C}_6\text{-D}^j$) it is concluded that the phosphorus atom is highly mobile. This is reflected in the small ¹H line widths of about 10 kHz in the aromatic region of

(47) Douglass, D. C.; McBrierty, V. J. *J. Chem. Phys.* **1971**, *54*, 4085.(48) Assink, R. A.; Wilkes, G. C. *Polym. Eng. Sci.* **1977**, *17*, 606.(49) Schmidt-Rohr, K.; Clauss, J.; Spiess, H. W. *Macromolecules* **1992**, *25*, 3273.

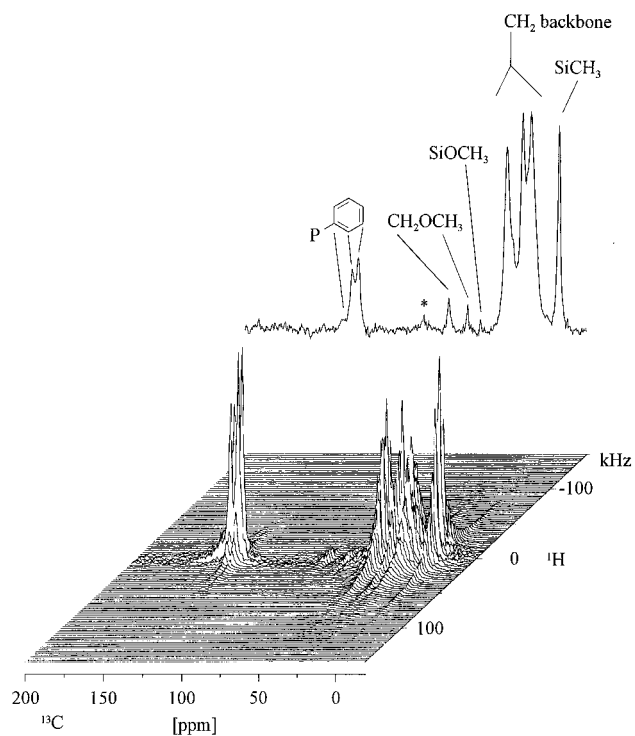


Figure 6. WISE spectrum of the polymer-bound ligand **2** (T^n)(D^i - C_6 - D^j) (bottom) and the corresponding ^{13}C CP/MAS NMR spectrum (top). Asterisks denote the spinning sidebands.

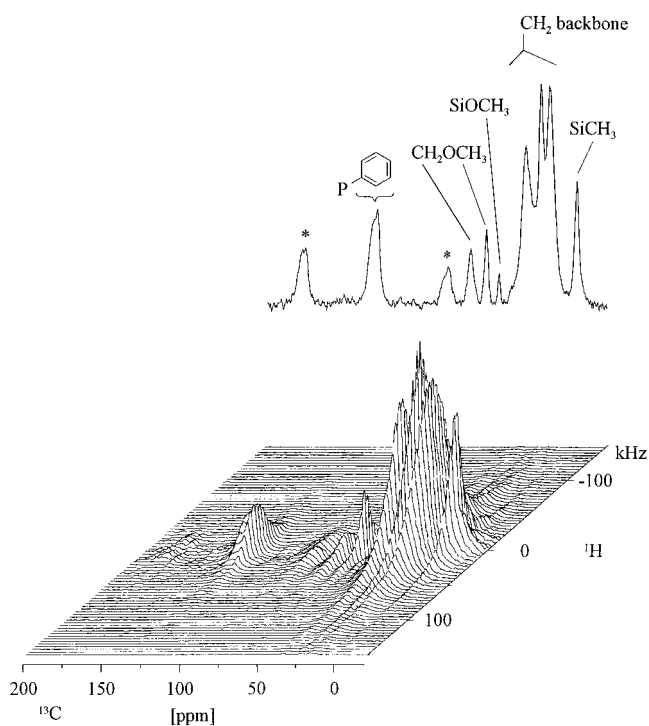


Figure 7. WISE spectrum of the polymer-bound ligand **3** (T^n) $_2$ (D^i - C_6 - D^j) $_2$ (bottom) and the corresponding ^{13}C CP/MAS NMR spectrum (top). Asterisks denote the spinning sidebands.

the WISE spectrum (Figure 6) which are narrower than those of the methylene groups (≈ 15 – 20 kHz) of the hydrocarbon backbone. Upon coordination of two polysiloxane-bound phosphine ligands to one rhodium to form the complex **3** (T^n) $_2$ (D^i - C_6 - D^j) $_2$, all resonances in the F1 dimension of the corresponding WISE spectrum (Figure 7) are broadened. The most significant changes of the line widths in the proton dimension are observed in the aromatic region (≈ 30 kHz) and for the methylene

groups between 10 and 40 ppm (≈ 40 – 50 kHz). These observations are consistent with the finding that the polysiloxane-bound complexes are more rigid than the corresponding polysiloxane-bound ligands even if only two ligands are anchored to the metal center. In the WISE spectrum of **3** (T^n) $_2$ (D^i - C_6 - D^j) $_2$ (Figure 7) the narrowest ^1H resonances (≈ 20 kHz) are observed for the methyl groups [OCH $_3$ and SiCH $_3$, see Figure 7] due to their fast rotation.

Surface Areas of the Materials. The surface area measurements according to the BET method revealed values between 0.1 and 2.8 m 2 /g for all samples (see Experimental Section). These low values are in the range of the external surface of the gel particles and agree well with the quantity (3 m 2 /g) obtained for the xerogel (D^i - C_6 - D^j) which was sol-gel processed with HCl as catalyst.¹⁹

Conclusion

The bis(silylated) D-functionalized matrix component precursors MeSi(OMe) $_2$ (CH $_2$) $_z$ (MeO) $_2$ SiMe [**1** (D^0 - C_z - D^0)] were successfully employed in the sol-gel process of the trimethoxysilyl functionalized ether-phosphine ligand PhP(CH $_2$ CH $_2$ OMe)(CH $_2$) $_3$ Si(OMe) $_3$ [**2** (T^0)] and its rhodium(I) complex ClRh(CO)(P~O) $_2$ [**3** (T^0) $_2$] to form a new class of functionalized organic-inorganic hybrid materials. Tuneable ratios of T/D as well as high degrees of cross-linkage of the D and T species were achieved which ensure a reduced leaching of functional groups from the matrix. In particular the washing out of the D groups was suppressed. The integrity of the complex coordination sphere and the carbon backbone was established by ^{13}C and ^{31}P CP/MAS NMR spectroscopy. The EXAFS spectroscopical study gave a more detailed insight into the structure of the local environment round the metal center of the complex **3** (T^n) $_2$. Solid-state NMR spectroscopic investigations of the polysiloxane-bound ether-phosphine ligands clearly demonstrate higher flexibilities of the D- C_z -D functionalized polysiloxanes compared to the Q-modified one. The highest mobility was found for the ligand **2** (T^n) (D^i - C_{14} - D^j), whereas the hexylene and octylene bridged analogues **2** (T^n) (D^i - C_6 - D^j) and **2** (T^n) (D^i - C_8 - D^j) displayed no significant differences in their mobilities. An additional cross-linkage of the matrix and therefore a strong restriction of the mobilities of the coordinating phosphorus atoms was obtained by the coordination of only two ligands to one rhodium center. 2D WISE NMR experiments which were exemplarily performed in the cases of the polymers **2** (T^n) (D^i - C_6 - D^j) and **3** (T^n) $_2$ (D^i - C_6 - D^j) $_2$ confirm this finding. However from the line widths of the ^{31}P resonances and the relaxation times of the co-condensed complexes, it is deduced that either extension of the flexible bridging group from hexylene to tetradecylene or increasing amounts (y) of D- C_6 -D result in enhanced dynamic properties of the phosphorus atoms and therefore of the complexes. From these points of view the D- C_z -D condensation agents can really act as network modifiers, which allows the control of the complex density and the flexibility of the polysiloxanes. Compared to the F-T/Q copolymers the D- C_z -D modified polysiloxane-bound complexes represent the more favorable stationary phases for the use in stoichiometric and catalytic interphase reactions. The low surface areas of the F-T/

D-C_z-D copolymers which could limit the accessibility of the reactive centers for substrates are compensated by sufficient swelling abilities of these materials. Experiments which demonstrate the reactivity of these supported metal complexes in catalytic and stoichiometric reactions are published elsewhere.⁵⁰

Experimental Section

The elemental analysis were carried out on a Carlo-Erba analyzer, Model 1106. IR data were obtained on a Bruker IFS 48 FT-IR spectrometer. The solution nuclear magnetic resonance spectra (NMR) were recorded on a Bruker DRX 250 spectrometer at 296 K. The frequencies and standards are as follows: ³¹P{¹H} NMR: 101.25 MHz, external 85% H₃PO₄ in acetone-*d*₆. ²⁹Si{¹H} NMR (DEPT45 pulse sequence): 49.69 MHz. ¹³C{¹H} NMR: 62.90 MHz. ¹H NMR: 250.13 MHz. The chemical shifts in the ¹³C{¹H}, ²⁹Si{¹H}, and ¹H NMR spectra were measured relative to partially deuterated solvent peaks which are reported relative to TMS. Mass spectra (field desorption) were acquired on a Finnigan MAT 711A modified by AMD Mess- und Datensysteme (8 kV, 30 °C) and reported as mass/charge (*m/z*).

The CP/MAS solid-state NMR spectra were recorded on a Bruker MSL 200 [²⁹Si] and a Bruker ASX 300 [¹³C and ³¹P] multinuclear spectrometer equipped with wide bore magnets (field strengths: 4.7 and 7.05 T). Magic angle spinning was applied at 3 kHz (²⁹Si), 5 kHz (³¹P), and 10–12 kHz (¹³C). All measurements were carried out under exclusion of molecular oxygen. Frequencies and standards: ²⁹Si, 39.75 MHz (Q8M8); ¹³C, 75.47 MHz [TMS, carbonyl resonance of glycine ($\delta = 176.03$) as the second standard]; ³¹P, 121.49 MHz [85% H₃PO₄, NH₄H₂PO₄ ($\delta = 0.8$) as the second standard]. The cross polarization constants *T*_{CH}, *T*_{PH}, and *T*_{SiH} were determined by variations of the contact time *T*_c (15–22 experiments). The proton relaxation time in the rotating frame was measured by direct proton spin lock- τ -CP experiments as described by Schaefer and Stejskal.⁴² *T*_{1P} and *T*_{1Si} values were received using the method developed by Torchia.⁵¹ The relaxation time data were obtained by using the Bruker software SIMFIT or Jandel software PEAKFIT. For quantification of the silyl species in all polysiloxanes, ²⁹Si CP/MAS NMR spectra at a contact time *T*_c of 4 ms were recorded by accumulating 6000–15000 fid's until acceptable signal/noise ratios were obtained. Peak deconvolution of the spectra was performed with the Bruker software XNMR using Voigtian line shapes. The relative amounts *I*₀ of each of the D⁰, D¹, D², T¹, T², and T³ species in one sample were calculated by inserting their peak areas of the deconvoluted spectra *I*(*T*_c), the individual *T*_{SiH} data, and the common *T*_{1ρH} value into eq 1.³⁶

$$I(T_c) = \frac{I_0}{(1 - T_{SiH}/T_{1\rho H})} (e^{-T_c/T_{1\rho H}} - e^{-T_c/T_{SiH}}) \quad (1)$$

Thereby the boundary condition *T*_{SiH} ≪ *T*_{1ρH} has to be considered.⁵² The WISE NMR spectra were recorded under MAS conditions (3.5 kHz). Fifty *t*₁ increments with a dwell time of 2–3 μs were used for each spectrum. Cross polarization was applied with contact times of 200 μs [**3**(T⁰)₂(D¹-C₆-D⁰)₂] and 300 μs [**2**(T⁰)(D¹-C₆-D⁰)]. For a more detailed description of other NMR parameters see ref 10.

The EXAFS measurements of **3**(T⁰)₂ were performed at the rhodium K-edge at 23224.0 eV at the beamline RÖMO II at the Hamburger Synchrotronstrahlungslabor (HASYLAB) at DESY, Hamburg, at 20 °C, using a Si(311) double-crystal monochromator under ambient conditions (5.4 GeV, beam current 50 mA). Data were collected in transmission mode with ion chambers. Energy calibration was monitored with a 20 μm thick rhodium metal foil. All measurements were

performed under an inert gas atmosphere. The sample itself was prepared by pressing a mixture of 200 mg of **3**(T⁰)₂ and 20 mg of polyethylene to a tablet of a diameter of 1.0 cm and a thickness of 2.5 mm.

Data were analyzed with a program package, specially developed for the requirements of amorphous samples, which is described in detail elsewhere.⁵³ The resulting EXAFS function was multiplied with *k*³ and Fourier filtered. The Fourier filtering range was 1.00–3.50 Å. Data analysis in *k* space was performed according to the curved wave multiple-scattering formalism with the program EXCURV90.⁵⁴ The mean free path of the scattered electrons was calculated from the imaginary part of the potential (VPI was set to -4.00), the amplitude reduction factor AFAC was fixed at 0.8, and an overall energy shift Δ*E*₀ was introduced to best fit the data. In the fitting procedure the coordination numbers were fixed at the known values which are corresponding to the ligands round the rhodium atom of **3**(T⁰)₂.

The surface areas were determined by analyzing the N₂ adsorption isotherms according to the BET method using a Micromeritics Gemini II. All manipulations were performed under argon by employing the usual Schlenk techniques. Methanol was dried with magnesium and distilled, ethanol was distilled from NaOEt. *n*-Hexane and toluene were distilled from sodium benzophenone ketyl. H₂O was distilled under inert gas prior to use. All solvents were stored under argon. The ether-phosphine **2**(T⁰)²⁷ and the starting complex *trans*-ClRh(CO)(PPh₃)₂²⁹ were synthesized as described previously.

Synthesis of the Monomeric Co-condensation Agents 1(D⁰-C_z-D⁰). The corresponding α,ω-alkadiene (Scheme 2) and the 2.5-fold amount of dichloromethylsilane were mixed at 0 °C in a round-bottom flask with a reflux condenser followed by addition of a solution of chloroplatinic acid in dry THF. The gentle autoreflux of the reaction mixture indicated the beginning of the hydrosilylation. The reaction was stirred at room temperature under argon until the vibration of the -C=C- double bond in the IR spectrum at 1640 cm⁻¹ disappeared (≈5 days). The volatiles were removed by evaporation under vacuum, and the residue was distilled to yield the intermediate α,ω-bis(dichloromethylsilyl)alkane. A dropwise addition of this α,ω-bis(dichloromethylsilyl)alkane to a cooled (0 °C) solution of NaOMe in methanol accomplished the synthesis. To complete the methanolysis the mixture was stirred at 60 °C for 1 h. NaCl and the solvent were removed by filtration (P2) and evaporation under vacuum, respectively. Distillation of the crude product under vacuum gave clear, analytical pure fluids.

1,6-Bis[(dimethoxy)methylsilyl]hexane [1(D⁰-C₆-D⁰)]. A mixture of 1,5-hexadiene (55 g, 670 mmol), dichloromethylsilane (193 g, 1.675 mol), and chloroplatinic acid in THF (1 mL of a 5.0 × 10⁻³ M solution) was stirred for 5 days. Distillation under vacuum afforded 158 g (76%) of 1,6-bis[(dichloro)methylsilyl]hexane: bp 140–150 °C/10 mbar. After methanolysis of this intermediate in a solution of NaOMe (110 g, 2.028 mol) in MeOH (500 mL) and distillation under vacuum a colorless liquid was obtained [yield of **1**(D⁰-C₆-D⁰): 66 g, 44%]; bp 95–105 °C; ¹H NMR (C₆D₆) δ 3.38 (s, 12H, SiOCH₃), 1.33–1.44 [m, 8H, SiCH₂(CH₂)₄CH₂Si], 0.61–0.67 [m, 4H, SiCH₂(CH₂)₄CH₂Si], 0.09 (s, 6H, SiCH₃); ¹³C{¹H} NMR (C₆D₆) δ 50.0 (SiOCH₃), 33.5 [Si(CH₂)₂CH₂CH₂(CH₂)₂Si], 23.3 [SiCH₂CH₂(CH₂)₂CH₂CH₂Si], 13.8 [SiCH₂CH₂(CH₂)₂CH₂CH₂-Si], -5.4 (SiCH₃); ²⁹Si{¹H} NMR (C₆D₆) δ -2.0. FD-MS *m/z* 294 (M⁺, 9), 105 [H₃CSi(OCH₃)₂, 100]. Anal. Calcd for C₁₂H₃₀O₄Si₂: C, 48.93; H, 10.27. Found: C, 48.53; H, 9.78.

1,8-Bis[(dimethoxy)methylsilyl]octane [1(D⁰-C₈-D⁰)]. A mixture of 1,7-octadiene (8.8 g, 80 mmol), dichloromethylsilane (22 g, 191 mmol), and chloroplatinic acid in THF (0.4 mL of 5.0 × 10⁻³ M solution) was stirred for 5 days. Distillation under vacuum afforded 14.6 g (54%) 1,8-bis[(dichloro)methylsilyl]octane: bp 110–120 °C. After methanolysis of this intermediate in a solution of NaOMe (10 g, 185 mmol) in

(50) Lindner, E.; Schneller, T.; Auer, F.; Wegner, P.; Mayer, H. A. *Chem. Eur. J.*, in press.

(51) Torchia, A. D. *J. Magn. Reson.* **1978**, *30*, 613.

(52) Harris, R. K. *Analyst* **1985**, *110*, 649.

(53) Ertel, T. S.; Bertagnolli, H.; Hückmann, S.; Kolb, U.; Peter, D. *Appl. Spectrosc.* **1992**, *46*, 690.

(54) Gurman, S. J.; Binsted, N.; Ross, I. *J. Phys. C* **1986**, *19*, 1845.

MeOH (125 mL) and distillation under vacuum a colorless liquid was obtained [yield of **1(D⁰-C₈-D⁰)**: 4.1 g, 30%]: bp 105–110 °C; ¹H NMR (C₆D₆) δ 3.39 (s, 12H, SiOCH₃), 1.28–1.44 [m, 12H, SiCH₂(CH₂)₆CH₂Si], 0.63 [m, 4H, SiCH₂(CH₂)₆CH₂-Si], 0.08 (s, 6H, SiCH₃); ¹³C {¹H} NMR (C₆D₆) δ 49.9 (SiOCH₃), 33.8 [Si(CH₂)₂CH₂(CH₂)₂CH₂(CH₂)₂Si], 29.8 [Si(CH₂)₃CH₂CH₂(CH₂)₃Si], 23.4 [SiCH₂CH₂(CH₂)₄CH₂CH₂Si], 13.8 [SiCH₂CH₂(CH₂)₄CH₂CH₂Si], -5.5 (SiCH₃); ²⁹Si {¹H} NMR (C₆D₆) δ -2.0. FD-MS *m/z* 322 (M⁺, 22), 291 [M⁺ - OCH₃, 8], 105 [H₃-CSi(OCH₃)₂, 100]. Anal. Calcd for C₁₄H₃₄O₄Si₂: C, 52.13; H, 10.62. Found: C, 51.95; H, 10.31.

1,14-Bis[(dimethoxy)methylsilyl]tetradecane [1(D⁰-C₁₄-D⁰). A mixture of 1,13-tetradecadiene (22.5 g, 116 mmol), dichloromethylsilane (33.5 g, 291 mmol), and chloroplatinic acid in THF (0.4 mL of a 5.0 × 10⁻³ M solution) was stirred for 5 days. Distillation under vacuum afforded 27 g (75%) 1,14-bis[(dichloro)methylsilyl]tetradecane: bp 150–170 °C. After methanolysis of this intermediate in a solution of NaOMe (20 g, 373 mmol) in MeOH (200 mL) and distillation under vacuum a colorless liquid was obtained [yield of **1(D⁰-C₁₄-D⁰)**: 11 g, 31%]: bp 140–160 °C; ¹H NMR (C₆D₆) δ 3.38 (s, 12H, SiOCH₃), 1.30–1.47 [m, 24H, SiCH₂(CH₂)₁₂CH₂Si], 0.66 [m, 4H, SiCH₂(CH₂)₁₂CH₂Si], 0.10 (s, 6H, SiCH₃); ¹³C {¹H} NMR (C₆D₆) δ 49.9 (SiOCH₃), 33.8 [Si(CH₂)₂CH₂(CH₂)₈CH₂(CH₂)₂Si], 29.9–30.2 [Si(CH₂)₃(CH₂)₈(CH₂)₃Si], 23.3 [SiCH₂CH₂(CH₂)₁₀CH₂CH₂Si], 13.7 [SiCH₂CH₂(CH₂)₁₀CH₂CH₂Si], -5.5 (SiCH₃); ²⁹Si {¹H} NMR (C₆D₆) δ -2.0. FD-MS *m/z* 406 (M⁺, 42), 375 [M⁺ - OCH₃, 8], 105 [H₃CSi(OCH₃)₂, 100]. Anal. Calcd for C₂₀H₄₆O₄Si₂: C, 59.06; H, 11.40. Found: C, 59.00; H, 11.14.

trans-Carbonylchlorobis[(2-methoxyethyl)phenyl(3-trimethoxysilyl)propyl]phosphine-Pt-rhodium(I) [3(T⁰)₂]. A suspension of **2(T⁰)** (153 mg, 0.463 mmol) and *trans*-ClRh(CO)(PPh₃)₂ (160 mg, 0.232 mmol) in toluene (20 mL) was stirred for 30 min at ambient temperature. After evaporation of the solvent under vacuum, the yellow oil was dissolved in *n*-pentane (10 mL), and the solution was allowed to stand 12 h at -30 °C to separate the products. This procedure was repeated to remove PPh₃ [yield of **3(T⁰)₂**: 176 mg, 92%]: ³¹P {¹H} NMR (CD₂Cl₂) δ 17.3 [d, ¹J_{RhP} 120 Hz]; ¹³C {¹H} NMR (CD₂Cl₂) δ 187.8 [dt, ¹J_{RhC} = 71, ²J_{PC} = 18 Hz, RhCO], 133.0 [vt, *N* = 13 Hz, ⁵⁵*i*-C_{arom}], 130.3–128.5 [m, *o*-, *m*-, *p*-C_{arom}], 69.4 (PCH₂CH₂OCH₃), 58.6 (CH₂OCH₃), 50.6 (SiOCH₃), 30.9 [vt, *N* = 25 Hz, ⁵⁵PCH₂CH₂OCH₃], 26.7 [vt, *N* = 25 Hz, ⁵⁵PCH₂CH₂CH₂Si], 18.6 (PCH₂CH₂CH₂Si), 11.4 [vt, *N* = 13 Hz, ⁵⁵CH₂Si]; IR (CH₂Cl₂, cm⁻¹) 1965 [ν(CO)]; FD-MS *m/z* 826 [M⁺ - H, 100]. Anal. Calcd for C₃₁H₅₄ClO₉P₂RhSi₂: C, 45.01; H, 6.58; Cl, 4.29. Found: C, 45.21; H, 6.58; Cl, 4.33.

Sol-Gel Processing. The monomers **1(D⁰-C_z-D⁰)** (*z* = 6, 8, 14) and mixtures of **2(T⁰)** and **3(T⁰)₂**, respectively, with specified quantities *y* of **1(D⁰-C_z-D⁰)** (*y* = 0, 1, 2, 4, 8, 16, 32 equiv), the 1.5-fold of the stoichiometric amount of water, and the catalyst (*n*-Bu)₂Sn(OAc)₂ was homogenized with a minimum amount of EtOH. The mixtures were sealed in a Schlenk tube and stirred for 12 h at ambient temperature until a gel was formed. Subsequently the solvent was removed under reduced pressure, and the gels were dried for 4 h. Solvent processing was performed by a vigorous stirring of the large gel particles in 40 mL of toluene (12 h), leading to sufficiently swollen gels. The wet gels were washed with another 40 mL volume of toluene, 40 mL of EtOH, and 40 mL of *n*-hexane and dried under vacuum (2 h). Final aging was carried out by drying the powders at 60 °C under vacuum for 8 h.

1,6-Bis(polymethylsiloxanyl)hexane [1(Dⁱ-C₆-D^j). A mixture of 1,6-bis[(dimethoxy)methylsilyl]hexane [**1(D⁰-C₆-D⁰)**] (747 mg, 2.536 mmol), water (137 mg, 7.61 mmol), and (*n*-Bu)₂Sn(OAc)₂ (27 mg, 0.077 mmol) in 1 mL of EtOH was sol-gel processed to give a colorless swollen gel. After solvent processing and aging a white powder was formed [yield of **1(Dⁱ-C₆-D^j)**: 503 mg, 98%]: ¹³C CP/MAS NMR δ 49.7 (SiOCH₃), 33.6 [Si(CH₂)₂CH₂CH₂(CH₂)₂Si, *T*_{CH} = 0.69 ms], 23.3 [SiCH₂CH₂(CH₂)₂CH₂CH₂Si, *T*_{CH} = 0.72 ms], 18.0 [SiCH₂CH₂(CH₂)₂CH₂CH₂Si, *T*_{CH} = 0.66 ms], -0.2 to -5.4 (SiCH₃,

*T*_{CH} = 0.85 ms); ²⁹Si CP/MAS NMR (silicon substructure) δ -2.2 (D⁰), -14.4 (D¹), -22.6 (D²). N₂ surface area: 2.3 m²/g. Anal. Calcd for C₈H₁₈O₂PSi₂ (idealized stoichiometry): C, 47.47; H, 8.96. Corrected stoichiometry:⁵⁶ C, 47.14; H, 8.98. Found: C, 46.03; H, 9.18.

1,8-Bis(polymethylsiloxanyl)octane [1(Dⁱ-C₈-D^j). A mixture of 1,8-bis[(dimethoxy)methylsilyl]octane [**1(D⁰-C₈-D⁰)**] (798 mg, 2.476 mmol), water (134 mg, 7.428 mmol), and (*n*-Bu)₂Sn(OAc)₂ (27 mg, 0.077 mmol) in 1 mL of EtOH was sol-gel processed to give a colorless swollen gel. After solvent processing and aging a white powder was formed [yield of **1(Dⁱ-C₈-D^j)**: 542 mg, 95%]: ¹³C CP/MAS NMR δ 49.7 (SiOCH₃), 33.6 [Si(CH₂)₂CH₂CH₂(CH₂)₂CH₂(CH₂)₂Si], 30.1 [Si(CH₂)₃CH₂CH₂(CH₂)₃Si], 23.4 [SiCH₂CH₂(CH₂)₄CH₂CH₂Si], 17.9 [SiCH₂CH₂(CH₂)₄CH₂CH₂Si], 0.03 to -5.3 (SiCH₃); ²⁹Si CP/MAS NMR (silicon substructure) δ -2.2 (D⁰), -14.5 (D¹), -22.6 (D²). N₂ surface area: 1.7 m²/g. Anal. Calcd for C₁₀H₂₂O₂Si₂ (idealized stoichiometry): C, 52.12; H, 9.62. Corrected stoichiometry:⁵⁶ C, 51.83; H, 9.63. Found: C, 51.93; H, 9.76.

1,14-Bis(polymethylsiloxanyl)tetradecane [1(Dⁱ-C₁₄-D^j). A mixture of 1,13-bis[(dimethoxy)methylsilyl]tetradecane [**1(D⁰-C₁₄-D⁰)**] (720 mg, 1.770 mmol), water (96 mg, 5.31 mmol), and (*n*-Bu)₂Sn(OAc)₂ (27 mg, 0.077 mmol) in 1 mL of EtOH was sol-gel processed to give a colorless swollen gel. After solvent processing and aging a white powder was formed [yield of **1(Dⁱ-C₁₄-D^j)**: 518 mg, 93%]: ¹³C CP/MAS NMR δ 49.5 (SiOCH₃), 33.6 [Si(CH₂)₂CH₂CH₂(CH₂)₈CH₂(CH₂)₂Si], 30.1 [Si(CH₂)₃(CH₂)₈(CH₂)₃Si], 23.3 [SiCH₂CH₂(CH₂)₁₀CH₂CH₂Si], 17.8 [SiCH₂CH₂(CH₂)₁₀CH₂CH₂Si], -0.15 (SiCH₃); ²⁹Si CP/MAS NMR (silicon substructure) δ -2.5 (D⁰), -12.4 (D¹), -22.6 (D²). N₂ surface area: 2.8 m²/g. Anal. Calcd for C₁₆H₃₄O₂Si₂ (idealized stoichiometry): C, 61.08; H, 10.89. Corrected stoichiometry:⁵⁶ C, 61.08; H, 10.90. Found: C, 61.39; H, 11.28.

(2-Methoxyethyl)phenyl(polysiloxanylpropyl)phosphine(Dⁱ-C₆-D^j) [2(T⁰)(Dⁱ-C₆-D^j). A mixture of the O,P ligand **2(T⁰)** (378 mg, 1.144 mmol), 1 equiv of **1(D⁰-C₆-D⁰)** (337 mg, 1.144 mmol), water (108 mg, 6.006 mmol), and (*n*-Bu)₂Sn(OAc)₂ (27 mg, 0.077 mmol) in 1 mL of EtOH was sol-gel processed to give a colorless gel. After solvent processing and aging a white powder was formed [yield of **2(T⁰)(Dⁱ-C₆-D^j)**: 493 mg, 93%]: ¹³C CP/MAS NMR δ 139.1 [*i*-C_{arom}], 132.4–128.5 [*o*-, *m*-, *p*-C_{arom}], 70.3 (PCH₂CH₂OCH₃), 58.0 (CH₂OCH₃), 49.8 (SiOCH₃), 33.1 [Si(CH₂)₂CH₂CH₂(CH₂)₂-Si], 26.9–17.8 [PCH₂CH₂CH₂Si, PCH₂CH₂OCH₃, Si(CH₂)₂CH₂CH₂(CH₂)₂Si], -0.2 to -5.3 (SiCH₃); ²⁹Si CP/MAS NMR (silicon substructure) δ -2.1 (D⁰), -13.0 (D¹), -22.2 (D²), -60.7 (T²), -67.9 (T³). N₂ surface area: 0.6 m²/g. Anal. Calcd for C₂₀H₃₆O_{4.5}PSi₃⁵⁷ (idealized stoichiometry): C, 51.80; H, 7.83. Corrected stoichiometry:⁵⁶ C, 50.85; H, 8.15. Found: C, 49.25; H, 7.99.

(2-Methoxyethyl)phenyl(polysiloxanylpropyl)phosphine(Dⁱ-C₈-D^j) [2(T⁰)(Dⁱ-C₈-D^j). A mixture of the O,P ligand **2(T⁰)** (365 mg, 1.105 mmol), 1 equiv of **1(D⁰-C₈-D⁰)** (356 mg, 1.105 mmol), water (104 mg, 5.805 mmol), and (*n*-Bu)₂Sn(OAc)₂ (27 mg, 0.077 mmol) in 1 mL of EtOH was sol-gel processed to give a colorless gel. After solvent processing and aging a white powder was formed [yield of **2(T⁰)(Dⁱ-C₈-D^j)**: 511 mg, 94%]: ¹³C CP/MAS NMR δ 139.1 [*i*-C_{arom}], 132.4–128.5 [*o*-, *m*-, *p*-C_{arom}], 70.3 (PCH₂CH₂OCH₃), 58.0 (CH₂OCH₃), 49.8 (SiOCH₃), 33.4 [Si(CH₂)₂CH₂(CH₂)₂CH₂(CH₂)₂Si], 29.7–17.7 [PCH₂CH₂CH₂Si, PCH₂CH₂OCH₃, Si(CH₂)₂CH₂(CH₂)₂CH₂(CH₂)₂Si], -0.1 (SiCH₃); ²⁹Si CP/MAS NMR (silicon substructure) δ -2.2 (D⁰), -14.1 (D¹), -22.3 (D²), -61.3 (T²), -68.0 (T³). N₂ surface area: 2.5 m²/g. Anal. Calcd for C₂₂H₄₀O_{4.5}PSi₃⁵⁷ (idealized stoichiometry): C, 53.73; H, 8.20. Corrected stoichiometry:⁵⁶ C, 53.17; H, 8.26. Found: C, 53.49; H, 8.65.

(2-Methoxyethyl)phenyl(polysiloxanylpropyl)phosphine(Dⁱ-C₁₄-D^j) [2(T⁰)(Dⁱ-C₁₄-D^j). A mixture of

(56) The corrected stoichiometry was obtained by adding the additional number of OH units of the D⁰, D¹, D², T¹, T², and T³ groups (obtained from the ²⁹Si CP/MAS NMR spectra) to the idealized stoichiometry (only D² and T³ units). The real T:D ratio and the degree of hydrolysis were also taken into account.

(57) The broken numbers in the chemical formulae are due to the SiO_{3/2} units or to the amount of T or D silicon units.

the O,P ligand **2(T⁰)** (379 mg, 1.147 mmol), 1 equiv of **1(D⁰-C₁₄-D⁰)** (467 mg, 1.147 mmol), water (108 mg, 6.006 mmol), and (*n*-Bu)₂Sn(OAc)₂ (27 mg, 0.077 mmol) in 1 mL of EtOH was sol-gel processed to give a colorless gel. After solvent processing and aging a white powder was formed [yield of **2(T⁰)(Dⁱ-C₁₄-Dⁱ)**: 588 mg, 89%]: ¹³C CP/MAS NMR δ 139.2 [*i*-C_{arom}], 132.4–128.4 [*o*-, *m*-, *p*-C_{arom}], 70.3 (PCH₂CH₂OCH₃), 58.0 (CH₂OCH₃), 49.7 (SiOCH₃), 33.4 [Si(CH₂)₂CH₂(CH₂)₈CH₂(CH₂)₂Si], 30.0–17.8 [PCH₂CH₂CH₂Si, PCH₂CH₂OCH₃, Si(CH₂)₂CH₂(CH)₈CH₂(CH₂)₂Si], -0.1 (SiCH₃); ²⁹Si CP/MAS NMR (silicon substructure) δ -12.2 (D¹), -22.3 (D²), -61.8 (T²), -68.0 (T³). N₂ surface area: 1.2 m²/g. Anal. Calcd for C₂₈H₅₂O_{4.5}PSi₃⁵⁷ (idealized stoichiometry): C, 58.39; H, 9.10. Corrected stoichiometry:⁵⁶ C, 57.83; H, 9.07. Found: C, 58.39; H, 9.27.

trans-Carbonylchlorobis[(2-methoxyethyl)phenyl(polysiloxanylpropyl)phosphine-P]rhodium(I)(Dⁱ-C₆-Dⁱ)₂ [3(T⁰)₂(Dⁱ-C₆-Dⁱ)₂]. A mixture of ClRh(CO)(P~O)₂ [3(T⁰)₂] (245 mg, 0.297 mmol), water (24 mg, 1.334 mmol), and (*n*-Bu)₂Sn(OAc)₂ (21 mg, 0.060 mmol) in 1 mL of EtOH was sol-gel processed to give a yellow gel [yield of **3(T⁰)₂**: 154 mg, 75%]: ¹³C CP/MAS NMR δ 187.5 (RhCO), 128.9 [*i*-, *m*-, *o*-, *p*-C_{arom}], 68.3 (PCH₂CH₂OCH₃), 58.1 (CH₂OCH₃), 50.1 (SiOCH₃), 27.3 (CH₂PCH₂), 18.2 (Si(CH₂)₂CH₂CH₂); ²⁹Si CP/MAS NMR (silicon substructure) δ -53.0 (T¹), -60.6 (T²), -67.4 (T³). IR (KBr, cm⁻¹) 1961 [ν(CO)]. N₂ surface area: 2.0 m²/g. Anal. Calcd for C₂₅H₃₆ClO₆P₂RhSi₂⁵⁷ (idealized stoichiometry): C, 43.58; H, 5.27; Cl, 5.14. Corrected stoichiometry:⁵⁶ C, 43.02; H, 5.34; Cl, 5.08. Found: C, 44.84; H, 5.88; Cl, 5.17.

trans-Carbonylchlorobis[(2-methoxyethyl)phenyl(polysiloxanylpropyl)phosphine-P]rhodium(I)(Dⁱ-C₆-Dⁱ)₂ [3(T⁰)₂(Dⁱ-C₆-Dⁱ)₂]. A mixture of ClRh(CO)(P~O)₂ [3(T⁰)₂] (265 mg, 0.320 mmol), 1 equiv of **1(D⁰-C₆-D⁰)** (94 mg, 0.320 mmol), water (43 mg, 2.398 mmol), and (*n*-Bu)₂Sn(OAc)₂ (27 mg, 0.077 mmol) in 1 mL of EtOH was sol-gel processed to give a yellow gel [yield of **3(T⁰)₂(Dⁱ-C₆-Dⁱ)₂**: 248 mg, 87%]: ¹³C CP/MAS NMR δ 129.6 [*i*-, *m*-, *o*-, *p*-C_{arom}], 67.7 (PCH₂CH₂OCH₃), 58.4 (CH₂OCH₃), 50.2 (SiOCH₃), 32.7 [Si(CH₂)₂CH₂CH₂(CH₂)₂Si], 23.3–17.8 [PCH₂CH₂CH₂Si, PCH₂CH₂OCH₃, Si(CH₂)₂CH₂CH₂(CH₂)₂Si], 0.3 (SiCH₃); ²⁹Si CP/MAS NMR (silicon substructure) δ -2.2 (D⁰), -13.4 (D¹), -22.4 (D²), -53.7 (T¹), -60.8 (T²), -67.3 (T³). IR (KBr, cm⁻¹) 1964 [ν(CO)]. N₂ surface area: 0.8 m²/g. Anal. Calcd for C₃₃H₅₄ClO₈P₂RhSi₄⁵⁷ (idealized stoichiometry): C, 44.46; H, 6.11; Cl, 3.98. Corrected stoichiometry:⁵⁶ C, 43.76; H, 5.97; Cl, 4.22. Found: C, 43.46; H, 6.54; Cl, 3.75.

trans-Carbonylchlorobis[(2-methoxyethyl)phenyl(polysiloxanylpropyl)phosphine-P]rhodium(I)(Dⁱ-C₆-Dⁱ)₂ [3(T⁰)₂(Dⁱ-C₆-Dⁱ)₂]. A mixture of ClRh(CO)(P~O)₂ [3(T⁰)₂] (609 mg, 0.736 mmol), 2 equiv of **1(D⁰-C₆-D⁰)** (433 mg, 1.472 mmol), water (139 mg, 7.723 mmol), and (*n*-Bu)₂Sn(OAc)₂ (27 mg, 0.077 mmol) in 1 mL of EtOH was sol-gel processed to give a yellow gel [yield of **3(T⁰)₂(Dⁱ-C₆-Dⁱ)₂**: 781 mg, 97%]: ³¹P CP/MAS NMR (line widths of the isotropic signal at different temperatures) ν_{1/2} [Hz] 1450 (294 K), 1376 (313 K), 1148 (333 K), 1041 (348 K); ¹³C CP/MAS NMR δ 187.3 (RhCO), 128.6 [*i*-, *m*-, *o*-, *p*-C_{arom}], 68.9 (PCH₂CH₂OCH₃), 58.1 (CH₂OCH₃), 49.9 (SiOCH₃), 33.1 [Si(CH₂)₂CH₂CH₂(CH₂)₂Si], 23.2–17.8 [PCH₂CH₂CH₂Si, PCH₂CH₂OCH₃, Si(CH₂)₂CH₂CH₂(CH₂)₂Si], -0.1 to -5.4 (SiCH₃); ²⁹Si CP/MAS NMR (silicon substructure) δ -1.9 (D⁰, T_{1Si} = 11.7 s), -13.7 (D¹, T_{1Si} = 15.3 s), -22.2 (D²), -53.7 (T¹), -59.6 (T², T_{1Si} = 61.4 s), -68.1 (T³). IR (KBr, cm⁻¹) 1964 [ν(CO)]. N₂ surface area: 1.6 m²/g. Anal. Calcd for C₄₁H₇₂ClO₁₀P₂RhSi₆⁵⁷ (idealized stoichiometry): C, 45.02; H, 6.63; Cl, 3.24. Corrected stoichiometry:⁵⁶ C, 44.53; H, 6.71; Cl, 3.20. Found: C, 43.76; H, 7.02; Cl, 3.30.

trans-Carbonylchlorobis[(2-methoxyethyl)phenyl(polysiloxanylpropyl)phosphine-P]rhodium(I)(Dⁱ-C₆-Dⁱ)₄ [3(T⁰)₂(Dⁱ-C₆-Dⁱ)₄]. A mixture of ClRh(CO)(P~O)₂ [3(T⁰)₂] (295 mg, 0.356 mmol), 4 equiv of **1(D⁰-C₆-D⁰)** (419 mg, 1.422 mmol), water (106 mg, 5.867 mmol), and (*n*-Bu)₂Sn(OAc)₂ (27 mg, 0.077 mmol) in 1 mL of EtOH was sol-gel processed to give a yellow gel [yield of **3(T⁰)₂(Dⁱ-C₆-Dⁱ)₄**: 486 mg, 91%]: ¹³C CP/MAS NMR δ 128.7 [*i*-, *m*-, *o*-, *p*-C_{arom}], 68.2 (PCH₂CH₂OCH₃), 58.0 (CH₂OCH₃), 49.9 (SiOCH₃), 33.5 [Si(CH₂)₂CH₂CH₂(CH₂)₂Si], 23.3–17.9 [PCH₂CH₂CH₂Si, PCH₂CH₂OCH₃, Si(CH₂)₂CH₂CH₂(CH₂)₂Si], 0.0 to -5.3 (SiCH₃); ²⁹Si CP/MAS NMR (silicon substructure) δ -2.2 (D⁰), -14.3 (D¹), -22.5 (D²), -60.2 (T²), -68.5 (T³). IR (Nujol mull, cm⁻¹) 1964 [ν(CO)]. N₂ surface area: 0.9 m²/g. Anal. Calcd for C₅₇H₁₀₈ClO₁₄P₂RhSi₁₀⁵⁷ (idealized stoichiometry): C, 45.68; H, 7.26; Cl, 2.37. Corrected stoichiometry:⁵⁶ C, 45.25; H, 7.31; Cl, 2.34. Found: C, 44.76; H, 7.67; Cl, 2.70.

trans-Carbonylchlorobis[(2-methoxyethyl)phenyl(polysiloxanylpropyl)phosphine-P]rhodium(I)(Dⁱ-C₆-Dⁱ)₈ [3(T⁰)₂(Dⁱ-C₆-Dⁱ)₈]. A mixture of ClRh(CO)(P~O)₂ [3(T⁰)₂] (218 mg, 0.264 mmol), 8 equiv of **1(D⁰-C₆-D⁰)** (622 mg, 2.112 mmol), water (136 mg, 7.529 mmol), and (*n*-Bu)₂Sn(OAc)₂ (27 mg, 0.077 mmol) in 1 mL of EtOH was sol-gel processed to give a yellow gel [yield of **3(T⁰)₂(Dⁱ-C₆-Dⁱ)₈**: 573 mg, 94%]: ¹³C CP/MAS NMR δ 128.4 [*i*-, *m*-, *o*-, *p*-C_{arom}], 68.6 (PCH₂CH₂OCH₃), 58.0 (CH₂OCH₃), 49.8 (SiOCH₃), 33.3 [Si(CH₂)₂CH₂CH₂(CH₂)₂Si], 23.2–17.9 [PCH₂CH₂CH₂Si, PCH₂CH₂OCH₃, Si(CH₂)₂CH₂CH₂(CH₂)₂Si], 0.1 to -5.5 (SiCH₃); ²⁹Si CP/MAS NMR (silicon substructure) δ -2.1 (D⁰), -14.1 (D¹), -22.4 (D²), -60.0 (T²), -68.9 (T³). IR (Nujol mull, cm⁻¹) 1967 [ν(CO)]. N₂ surface area: 0.6 m²/g. Anal. Calcd for C₈₉H₁₈₀ClO₂₂P₂RhSi₁₈⁵⁷ (idealized stoichiometry): C, 46.31; H, 7.86; Cl, 1.54. Corrected stoichiometry:⁵⁶ C, 45.80; H, 7.91; Cl, 1.51. Found: C, 44.83; H, 8.13; Cl, 1.51.

trans-Carbonylchlorobis[(2-methoxyethyl)phenyl(polysiloxanylpropyl)phosphine-P]rhodium(I)(Dⁱ-C₆-Dⁱ)₁₆ [3(T⁰)₂(Dⁱ-C₆-Dⁱ)₁₆]. A mixture of ClRh(CO)(P~O)₂ [3(T⁰)₂] (283 mg, 0.342 mmol), 16 equiv of **1(D⁰-C₆-D⁰)** (1.612 g, 5.472 mmol), water (323 mg, 17.955 mmol), and (*n*-Bu)₂Sn(OAc)₂ (27 mg, 0.077 mmol) in 1 mL of EtOH was sol-gel processed to give a slightly yellow gel [yield of **3(T⁰)₂(Dⁱ-C₆-Dⁱ)₁₆**: 1.316 g, 98%]: ¹³C CP/MAS NMR δ 128.4 [*i*-, *m*-, *o*-, *p*-C_{arom}], 69.2 (PCH₂CH₂OCH₃), 57.9 (CH₂OCH₃), 49.7 (SiOCH₃), 33.3 [Si(CH₂)₂CH₂CH₂(CH₂)₂Si], 23.2–17.9 [PCH₂CH₂CH₂Si, PCH₂CH₂OCH₃, Si(CH₂)₂CH₂CH₂(CH₂)₂Si], 0.2 to -5.6 (SiCH₃); ²⁹Si CP/MAS NMR (silicon substructure) δ -2.1 (D⁰), -14.2 (D¹), -22.7 (D²), -61.0 (T²), -69.4 (T³). IR (Nujol mull, cm⁻¹) 1966 [ν(CO)]. N₂ surface area: 1.4 m²/g. Anal. Calcd for C₁₅₃H₃₂₄ClO₃₈P₂RhSi₃₄⁵⁷ (idealized stoichiometry): C, 46.79; H, 8.39; Cl, 0.90. Corrected stoichiometry:⁵⁶ C, 46.49; H, 8.39; Cl, 0.83. Found: C, 45.75; H, 8.90; Cl, 0.78.

trans-Carbonylchlorobis[(2-methoxyethyl)phenyl(polysiloxanylpropyl)phosphine-P]rhodium(I)(Dⁱ-C₆-Dⁱ)₃₂ [3(T⁰)₂(Dⁱ-C₆-Dⁱ)₃₂]. A mixture of ClRh(CO)(P~O)₂ [3(T⁰)₂] (270 mg, 0.326 mmol), 32 equiv of **1(D⁰-C₆-D⁰)** (3.068 g, 10.416 mmol), water (589 mg, 32.710 mmol), and (*n*-Bu)₂Sn(OAc)₂ (27 mg, 0.077 mmol) in 1 mL of EtOH was sol-gel processed to give a slightly yellow gel [yield of **3(T⁰)₂(Dⁱ-C₆-Dⁱ)₃₂**: 2.079 g, 89%]: ¹³C CP/MAS NMR δ 128.7 [*i*-, *m*-, *o*-, *p*-C_{arom}], 67.9 (PCH₂CH₂OCH₃), 57.9 (CH₂OCH₃), 49.8 (SiOCH₃), 33.4 [Si(CH₂)₂CH₂CH₂(CH₂)₂Si], 23.2–17.9 [PCH₂CH₂CH₂Si, PCH₂CH₂OCH₃, Si(CH₂)₂CH₂CH₂(CH₂)₂Si], 0.2 to -5.5 (SiCH₃); ²⁹Si CP/MAS NMR (silicon substructure) δ -1.9 (D⁰), -14.4 (D¹), -22.7 (D²), -60.0 (T²), -69.0 (T³). IR (Nujol mull, cm⁻¹) 1968 [ν(CO)]. N₂ surface area: 0.7 m²/g. Anal. Calcd for C₂₈₁H₆₁₂ClO₇₀P₂RhSi₆₆⁵⁷ (idealized stoichiometry): C, 47.10; H, 8.61; Cl, 0.49. Corrected stoichiometry:⁵⁶ C, 46.57; H, 8.63; Cl, 0.51. Found: C, 46.13; H, 9.81; Cl, 0.39.

trans-Carbonylchlorobis[(2-methoxyethyl)phenyl(polysiloxanylpropyl)phosphine-P]rhodium(I)(Dⁱ-C₈-Dⁱ)₂ [3(T⁰)₂(Dⁱ-C₈-Dⁱ)₂]. A mixture of ClRh(CO)(P~O)₂ [3(T⁰)₂] (620 mg, 0.749 mmol), 2 equiv of **1(D⁰-C₈-D⁰)** (483 mg, 1.498 mmol), water (142 mg, 7.865 mmol), and (*n*-Bu)₂Sn(OAc)₂ (27 mg, 0.077 mmol) in 1 mL of EtOH was sol-gel processed to give a yellow gel [yield of **3(T⁰)₂(Dⁱ-C₈-Dⁱ)₂**: 818 mg, 95%]: ¹³C CP/MAS NMR δ 128.7 [*i*-, *m*-, *o*-, *p*-C_{arom}], 68.2 (PCH₂CH₂OCH₃), 58.1 (CH₂OCH₃), 49.9 (SiOCH₃), 33.4 [Si(CH₂)₂CH₂(CH₂)₂Si], 29.7–17.7 [PCH₂CH₂CH₂Si, PCH₂CH₂OCH₃, Si(CH₂)₂CH₂(CH₂)₂Si], 0.2 to -5.5 (SiCH₃); ²⁹Si CP/MAS NMR (silicon substructure) δ -2.1 (D⁰), -13.1 (D¹), -22.3 (D²), -51.9 (T¹), -60.0 (T²), -68.3 (T³). IR (KBr, cm⁻¹) 1965 [ν(CO)]. N₂ surface area: 0.7 m²/g. Anal. Calcd for C₄₅H₈₀ClO₁₀P₂RhSi₆⁵⁷ (idealized stoichiometry): C, 47.00; H, 7.01; Cl, 3.08. Corrected stoichiometry:⁵⁶ C, 46.43; H, 7.01; Cl, 3.11. Found: C, 46.83; H, 7.48; Cl, 2.97.

trans-Carbonylchlorobis[(2-methoxyethyl)phenyl(polysiloxanylpropyl)phosphine-*P*]rhodium(I)(Dⁱ-C₁₄-D^j)₂ [3(Tⁿ)₂(Dⁱ-C₁₄-D^j)₂]. A mixture of ClRh(CO)(P~O)₂ [3(T⁰)₂] (421 mg, 0.509 mmol), 2 equiv of 1(D⁰-C₁₄-D⁰) (414 mg, 1.018 mmol), water (76 mg, 4.199 mmol), and (*n*-Bu)₂Sn(OAc)₂ (27 mg, 0.077 mmol) in 1 mL of EtOH was sol-gel processed to give a yellow gel [yield of 3(Tⁿ)₂(Dⁱ-C₁₄-D^j)₂: 664 mg, 99%]: ¹³C CP/MAS NMR δ 128.9 [*i*-, *m*-, *o*-, *p*-C_{arom}], 68.2 (PCH₂CH₂OCH₃), 58.1 (CH₂OCH₃), 49.9 (SiOCH₃), 30.1–17.8 [PCH₂CH₂CH₂Si, PCH₂CH₂OCH₃, Si(CH₂)₁₄Si], -0.1 (SiCH₃); ²⁹Si CP/MAS NMR (silicon substructure) δ -2.1 (D⁰), -14.1 (D¹), -22.4 (D²), -49.4 (T¹), -60.4 (T²), -67.7 (T³). IR (Nujol mull, cm⁻¹) 1961 [ν(CO)]. N₂ surface area: 0.1 m²/g. Anal. Calcd for C₅₇H₁₀₄ClO₁₀P₂RhSi₆⁵⁷ (idealized stoichiometry): C, 51.93; H, 7.95; Cl, 2.69. Corrected stoichiometry:⁵⁶ C, 51.35; H, 7.91; Cl, 2.74. Found: C, 51.44; H, 8.28; Cl, 2.79.

Acknowledgment. The support of this research by the Deutsche Forschungsgemeinschaft (Forschergruppe, Grant No. Li 154/41-3) Bonn/Bad Godesberg, and by the Fonds der Chemischen Industrie, Frankfurt/Main is gratefully acknowledged. We are grateful to Degussa AG, Germany for a generous gift of RhCl₃·H₂O and to Wacker Chemie GmbH for a generous gift of HSi(Me)-Cl₂. We thank Prof. K. G. Nickel, Institut für Mineralogie, University of Tübingen and Dipl.-Chem. W. Wielandt, Institut für Anorganische Chemie, University of Tübingen, for BET measurements.

CM960570R